NAVAL POSTGRADUATE SCHOOL
Monterey, California

PERFORMANCE OF A DUCTED MICRO-TURBOJET ENGINE

by

Loukas Andreou

September 1999

Thesis Advisor:	Garth V. Hobson
Second Reader:	Raymond P. Shreeve

Approved for public release; distribution is unlimited.

(i) REPORT DOCUMENTATION PAGE

Form Approved OMB No. 0704-0188

1. AGENCY USE ONLY ***(Leave blank)***

2. REPORT DATE
September 1999

3. REPORT TYPE AND DATES COVERED
Master's Thesis

4. TITLE AND SUBTITLE
PERFORMANCE OF A DUCTED MICRO-TURBOJET ENGINE

5. FUNDING NUMBERS

6. AUTHOR(S)
Loukas Andreou

7. PERFORMING ORGANIZATION NAME(S) AND ADDRESS(ES)
Naval Postgraduate School
Monterey, CA 93943-5000

8. PERFORMING ORGANIZATION REPORT NUMBER

9. SPONSORING / MONITORING AGENCY NAME(S) AND ADDRESS(ES)

10. SPONSORING / MONITORING AGENCY REPORT NUMBER

11. SUPPLEMENTARY NOTES
The views expressed in this thesis are those of the author and do not reflect the official policy or position of the Department of Defense or the U.S. Government.

12a. DISTRIBUTION / AVAILABILITY STATEMENT
Approved for public release; distribution is unlimited.

12b. DISTRIBUTION CODE

ABSTRACT ***(maximum 200 words)*** A turbo-ramjet engine configuration has possible applications in missiles or Uninhabited Aerial Vehicle's (UAV's). In order to study possible configurations, a Sophia J450 turbojet engine was used, with varying shroud configurations, to compare static thrust and specific fuel consumption measured in a test rig. A baseline shroud, which covered the engine, was tested with three ducts lengths aft of the J450's exhaust. Each duct length was tested with and without the final convergent nozzle. An elliptic intake for the shroud was also manufactured and tested on two of the configurations. Shroud pressures were also recorded to determine the amount of entrainment of secondary flow into the shroud. The short shroud was found to produce the best performance of the three configurations tested.

14. SUBJECT TERMS
Micro-Turbojet, GASTURB, Engine Shroud, Turboramjet, Sophia J450, Microturbine Performance

15. NUMBER OF PAGES
92

16. PRICE CODE

17. SECURITY CLASSIFICATION OF REPORT	18. SECURITY CLASSIFICATION OF THIS PAGE	19. SECURITY CLASSIFICATION OF ABSTRACT	20. LIMITATION OF ABSTRACT
Unclassified	Unclassified	Unclassified	UL

NSN 7540-01-280-5500

Standard Form 298 (Rev. 2-89)
Prescribed by ANSI Std. 239-18

THIS PAGE INTENTIONALLY LEFT BLANK

Approved for public release; distribution is unlimited

PERFORMANCE OF A DUCTED MICRO-TURBOJET ENGINE

Loukas Andreou
Lieutenant, Hellenic Navy
B.S.M.E., Hellenic Naval Academy, 1987

Submitted in partial fulfillment of the requirements for the degree of

MASTER OF SCIENCE IN AERONAUTICAL ENGINEERING

from the

NAVAL POSTGRADUATE SCHOOL
September 1999

Author: ______________________
Loukas Andreou

Approved by: ______________________
Garth V. Hobson, Thesis Advisor

____
Raymond P. Shreeve, Second Reader

____
Gerald H. Lindsey, Chairman, Department of
Aeronautics and Astronautics

THIS PAGE INTENTIONALLY LEFT BLANK

ABSTRACT

A turbo-ramjet engine configuration has possible applications in missiles or uninhabited aerial vehicles (UAV's). In order to study possible configurations, a Sophia J450 turbojet engine was used, with varying shroud configurations, to compare static thrust and specific fuel consumption measured in a test rig. A baseline shroud, which covered the engine, was tested with three ducts lengths aft of the J450's exhaust. Each duct length was tested with and without a final convergent nozzle. An elliptic intake for the shroud was also manufactured and tested on two of the configurations. Shroud pressures were also recorded to determine the amount of entrainment of secondary flow into the shroud. The short shroud was found to produce the best performance of the three configurations tested.

THIS PAGE INTENTIONALLY LEFT BLANK

TABLE OF CONTENTS

ACKNOWLEDGEMENTS

I extend my sincere appreciation in acknowledging several persons whose efforts greatly contributed towards the development of this thesis.

I would like to thank Mr. Rick Still , Mr. John Gibson, and Mr. Doug Seivwright of the Department of Aeronautics and Astronautics.

I greatly appreciate the efforts of Dr. Garth Hobson in providing the opportunity to pursue this thesis. Without his guidance, patience, and dedicated support, this research would never have been completed.

I would also like to thank my wife, Artemis, her passion and support were never ending even through pregnancy and motherhood.

I. INTRODUCTION

The attraction of the gas turbine engine for aircraft propulsion is its large power output in relation to the engine weight and size. It was this which led to the rapid development of the jet engine since the Second World War and the pioneering days of von Ohain and Whittle.

Since then, these engines have primarily grown larger in order to meet the increasing demand of thrust, at reduced fuel consumption. In more recent times, however, the popularity of remotely-controlled airplanes has created a new demand for scaled-down aircraft and jet engines. For this reason the potential of the Uninhabited Aerial Vehicle (UAV) in reconnaissance as well as strike roles has been recognized. Small expendable turbojet engines may also provide the necessary gas generator core for turbo-ramjet engines, which could be used to power supersonic UAVs. The supersonic propulsion of UAV's with turbo-ramjet engines forms the motivation for this thesis.

In 1998, Rivera (Ref.1), began testing the compressor performance of a Garrett T2 turbocharger. This turbocharger was similar to the rotor used in the Sophia J450 turbojet engine. He also bench tested the Sophia J450, and compared the results to previously documented tests conducted on another small turbojet engine tested by Lobik (Ref. 2), the JPX-240. Rivera also investigated the on- and off-design performance prediction of the Sophia J450 turbojet engine using a cycle analysis program GASTURB (Ref. 3), incorporating the experimentally determined Garrett T2 compressor map. The performance predictions were then favorably compared to off-design tests of the Sophia J450.

Hackaday (Ref. 4), performed a study of the static performance of the Sophia J450 with a non-optimized constant area ejector. These results were compared to baseline engine measurements obtained by Rivera to evaluate thrust augmentation. The results were also compared to theoretical predications obtained using a one-dimensional analysis of the ejector flow. The compressor map for the actual rotor within the J450 was obtained and used with GASTURB to better predict the Sophia's off-design performance. Then an engine shroud was constructed and measurements were made as an initial setup in the consideration of a combined cycle engine.

In the present study a Sophia J450 turbojet engine was used with varying shroud and duct configurations, to compare the performance of different duct lengths. Pressure measurements were also performed along the length of the various duct configurations to determine the amount of secondary flow entrainment into the shroud. An elliptical engine intake was designed and tested with two of the shroud configurations.

II. SOPHIA J450 ENGINE TEST PROGRAM

A. EXPERIMENTAL SETUP

1. Overview

The Japanese-built Sophia J450 turbojet was a small jet engine manufactured primarily for use in remotely-controlled model airplanes. The Sophia used heavy fuels which was either jet fuel or a kerosene/Coleman lantern fuel mixture. The J450 required an electric fuel pump, which delivered 85 psi. maximum pressure, and was powered by a variable-current 12V supply.

2. Engine Test Rig

The engine test rig used for the Sophia J450 was located in the Gas Dynamics Laboratory (Building 216) at the Naval Postgraduate School. A schematic of the test rig components are shown below in Figure 1.

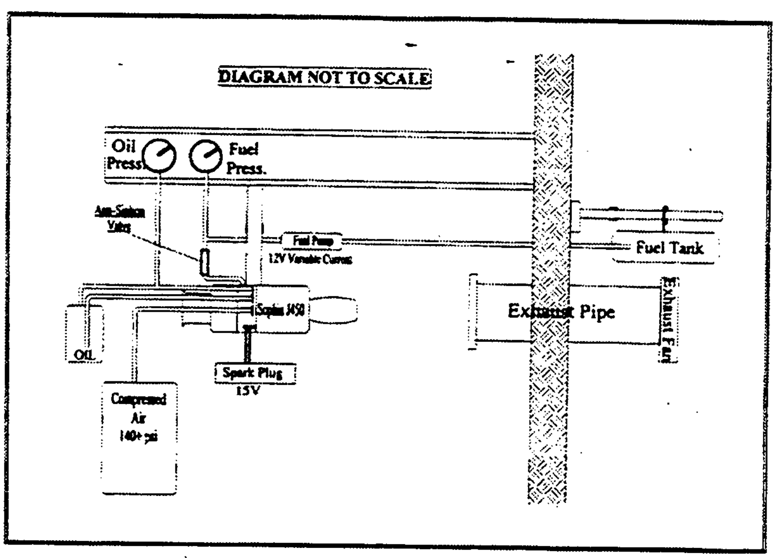

Figure 1. Engine Test Rig

Two pressure gages were mounted on the test rig I-beam. Sophia provided the fuel pressure gage, range 0-85 psig (0 - 6 kg/cm^2), which was connected to the fuel supply line by flexible tubing and provided readings of the fuel pressure supplied to the engine. The oil pressure gage, ranged 0-23.5 psig (0 - 1.6 bars), was connected to the engine compressor pressure port by flexible tubing. The compressor pressure port also pressurized the oil tank, which fed oil to the two engine bearings.

3. Shroud and Duct Configurations

Figure 2 is a schematic of the engine in its shroud. The configuration shown is the long shroud which included all the straight duct sections A through C. Six main configurations were tested. The first configuration was the engine only with the bellmouth, for mass flow rate measurement, attached as shown in Figure A-1, Appendix A. Next was the engine with its flight intake or cowling as shown in Figure 2. The third configuration tested was the engine with intake installed inside the baseline shroud. This included the first three duct sections shown in Figure 2, with the inlet to the duct at the same axial plane as the inlet to the J450, and the final section ended after duct section A in Figure 2. The fourth configuration tested was the short shroud which only had straight sections A and B attached to the shroud. This configuration was tested with and without the final nozzle section. The fifth configuration tested was the medium shroud, which included only duct sections B and C (with A removed). This configuration was tested with and without the final nozzle, and with the elliptical intake attached to the shroud. The final configuration tested was the long shroud as shown in Figure 2. This too was tested with and without the final nozzle, and was also tested with and without the elliptic intake.

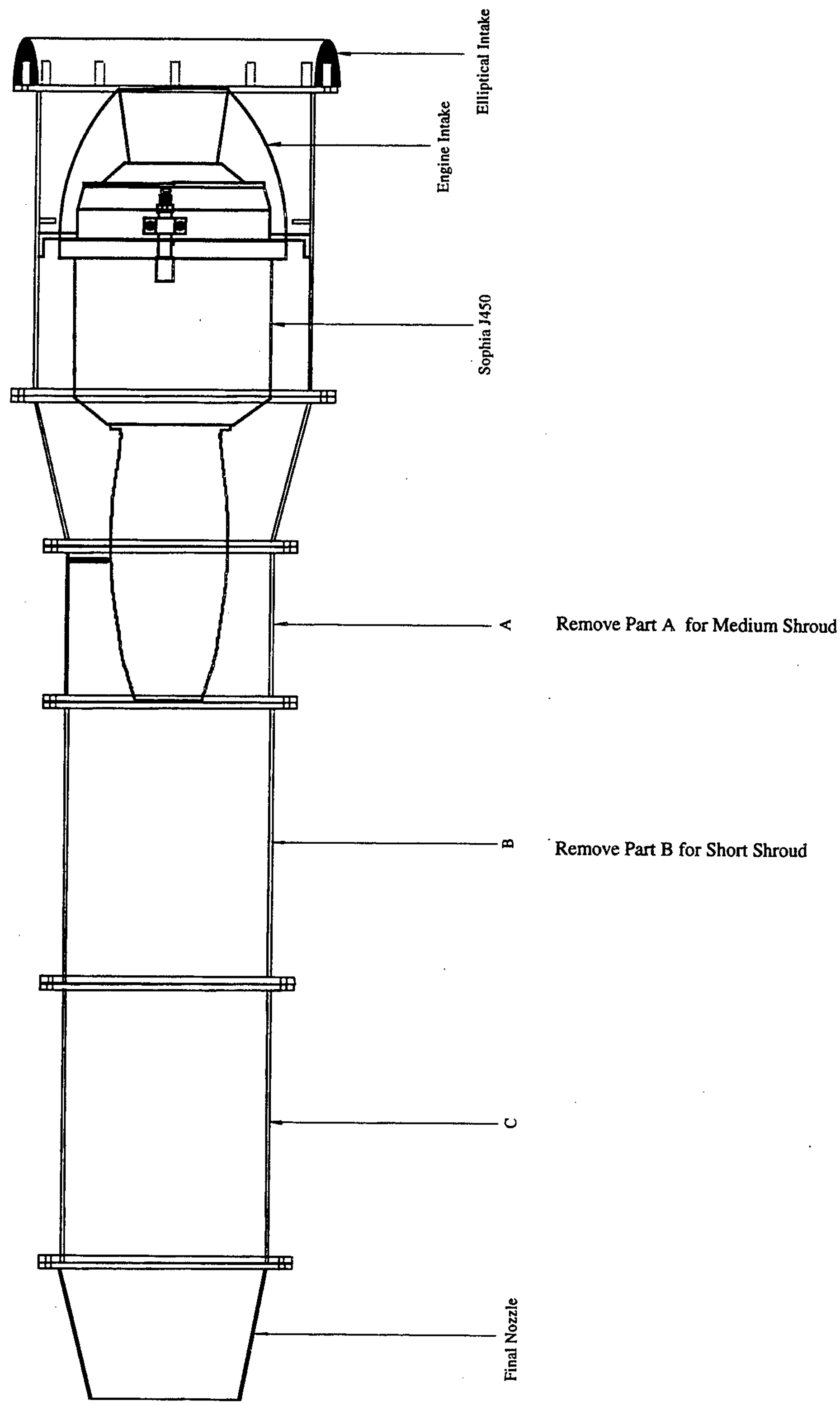

Figure 2. Long Shroud with Nozzle

Figure 3a is a digital picture of the front of the engine inside the short shroud installed in the test stand. The front view also shows the engine intake (or cowling), and in the lower left-hand corner is shown the oil tank and fuel pump. Figure 3b is a rear view of the short shroud and the final nozzle, showing the pressure taps on the shroud. Also shown is the bank of water manometers on the left and the fuel pump on the right.

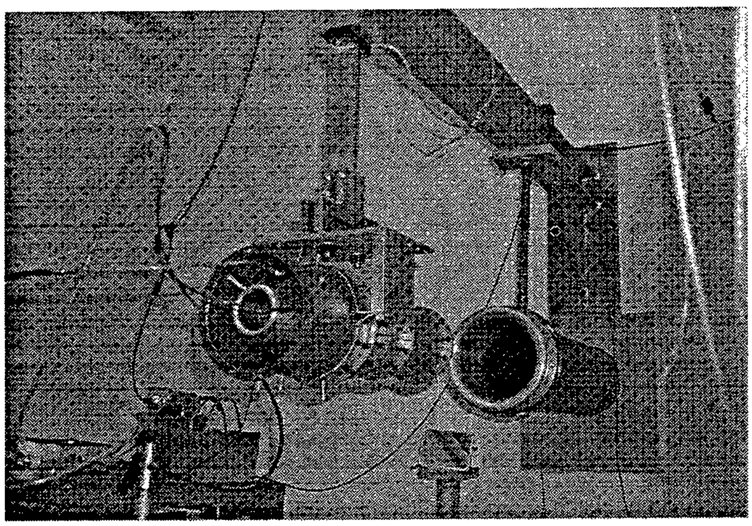

Figure 3a. Front View of Shroud with Engine

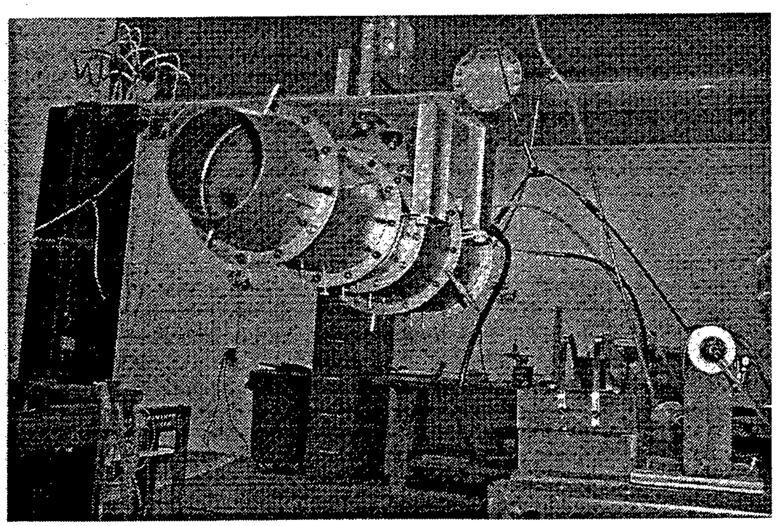

Figure 3b. Rear View of Shroud

B. DATA ACQUISITION AND REDUCTION

1. Overview

A HP9000 Series 300 workstation was used to control the data acquisition system, as well as store and process the data. The primary sensors used for data acquisition were strain gages and pressure taps. The strain readings were obtained with a HP3497A Data Acquisition Control Unit (DACU) in conjunction with a HP digital voltmeter (DVM), which measured strain-gage voltage after signal conditioning. Pressures were sensed using the Scanivalve Zero-Operate-Calibrate (ZOC-14) system in conjunction with the CALSYS 2000 calibration standard. The ZOC-14 and CALSYS systems were controlled by the workstation using the HP6944A Multiprogrammer. The DACU, DVM, CALSYS, and multiprogrammer were connected to the workstation via an HP-IB (IEEE-488) BUS. The test rig data acquisition is shown schematically in Figure 4.

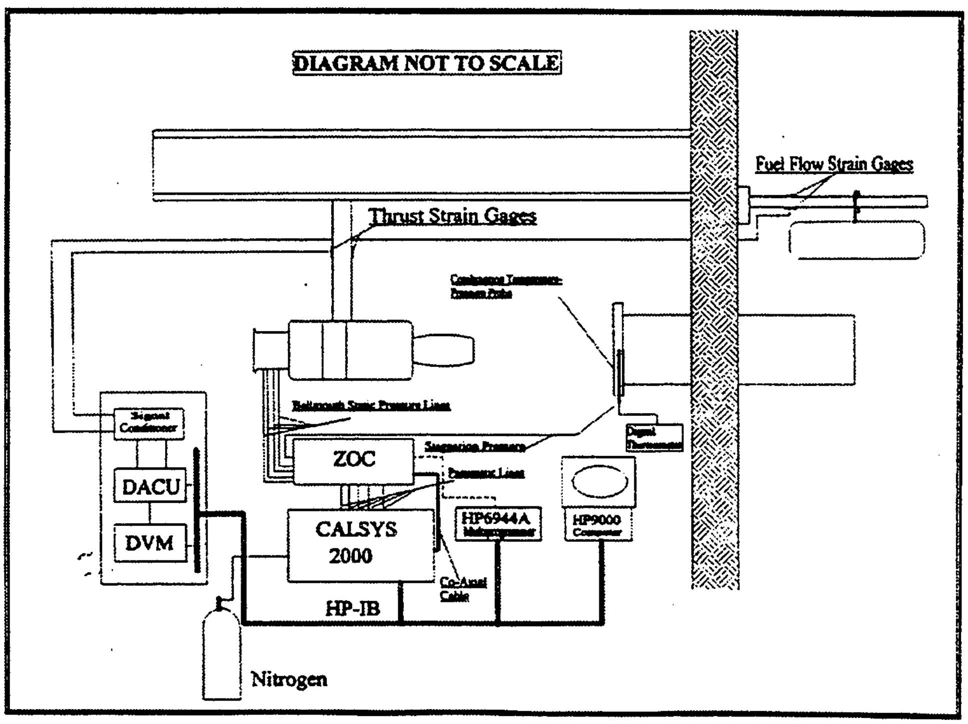

Figure 4. Engine Test Rig Data Acquisition Schematic

2. Instrumentation and Control

a) Thrust Measurements

Thrust measurements were accomplished by use of strain gages placed on the suspension beam used to support the engine. The strain gauges were placed in a full Wheatstone bridge configuration that fed their signals to a signal conditioner cued by the HP3497A Data Acquisition Control Unit (DACU). The Digital Voltmeter (DVM) was also used to zero out the bridge prior to performing the calibration through channel five on the front panel of the signal conditioner. A pre- and post calibration was performed, and the results are located in Appendix J. Care was taken to ensure that the thrust beam was at the center of the gravity of each engine configuration. Center of gravity calculations were performed for the different engine configurations and the results are given in Appendix I.

b) Fuel Flow Rate Measurements

The fuel flow rate was determined by using a cantilevered beam as a weighing device to calculate the change in fuel weight over a given period of time. The output of the P-3500 strain-gauge unit was fed to channel zero of the signal conditioner. A pre- and post calibration was performed and the results are given in Appendix J.

c) Mass Flow Rate Measurements

Pressure measurements were taken from the four pressure taps placed ninety degrees from one another on the bellmouth. The sample pressures are taken utilizing the Scanivalve ZOC system. With the average static pressure known, the average mass flow rate into the engine was calculated using equation 10 in Ref. 1.

d) Shroud Pressures

These were recorded with a bank of eleven water manometers. ZOC measurements were also attempted but these proved unreliable since the entrainment pressures were too low for the 50 psi transducer in the ZOC array. The location of the pressure taps can be seen in Figure A-5 (Appendix A).

e) Exhaust Gas Temperature

Exhaust gas temperature was measured with a hand-held HH-21/23 Microprocessor Digital Thermometer, for the medium and long shroud configurations. The tabulated temperatures at varying engine speeds are presented in Appendix D. The thermocouple used in the exhaust gas stream was a J-type Chromel-Alumel thermocouple.

f) Engine RPM

Engine RPM was verified using a new Sophia J450 engine, as can be seen in Table 1. The engine was fitted with a laser diode and optical sensor in the compressor nut. The engine RPM was recorded with the Ground System Unit (GSU) supplied by Sophia.

% SPOOL SPEED	RPM	PRESSURE (bar)
80	92,000	0.65
90	103,500	0.9
100	115,000	1.15
105	121,000	1.3

Table 1. Pressure/RPM Table

3. Software

The programs MICROJET_CAL, MICROJET, and READ_MJ_ZOC were used to calibrate the data acquisition system, record data and process the raw data. These programs are explained in detail by Rivera (Ref. 1).

C. RESULTS OF TEST PROGRAM

As mentioned previously, six major engine configurations were tested; namely, (1) the engine with bellmouth, (2) the engine with its flight intake, (3) the baseline shroud covering the engine and (4) short, (5) medium and (6) long shroud lengths. The medium and long shroud lengths were each tested with and without the elliptic intake on the engine shroud. For each test, thrust and specific fuel consumption (SFC) were determined at various speeds from 80% to 105% of design rotor speed.

1. Bell Mouth Configuration

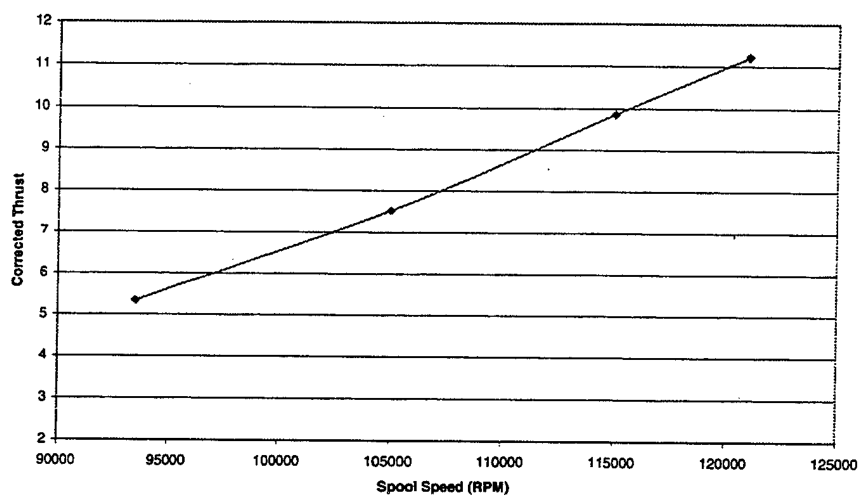

Figure 5a. Thrust Measurements

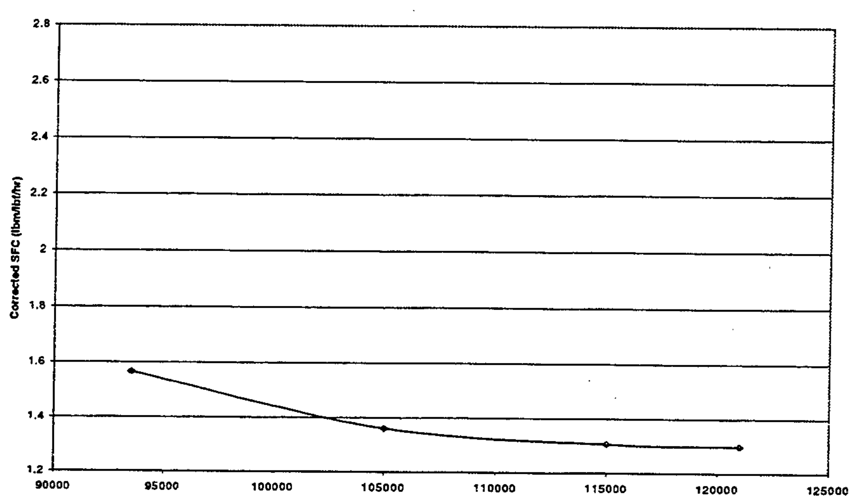

Figure 5b. SFC Measurements

For the bellmouth configuration it can be noted in Figure 5a that the engine spool speed in revolutions per minute (RPM) had a very large effect on the thrust, and the variation as speed increased was almost linear. From 80% spool speed to 100% spool speed the thrust output increased almost 5 lbf, or doubled in value. In comparison, as the spool speed was increased, the SFC decreased steadily as can be seen in Figure 5b. From 100% to 105% spool speed it was noted that the SFC was almost constant.

2. Engine Intake Configuration

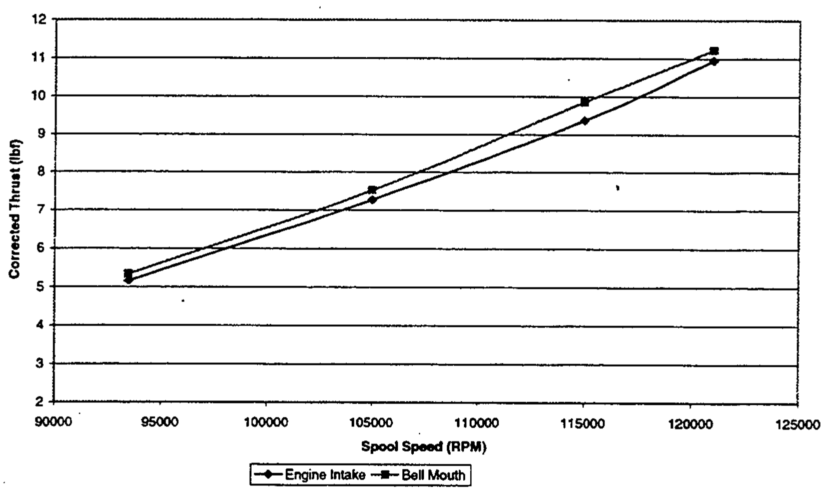

Figure 6a. Thrust Comparison; Engine Intake vs. Bellmouth

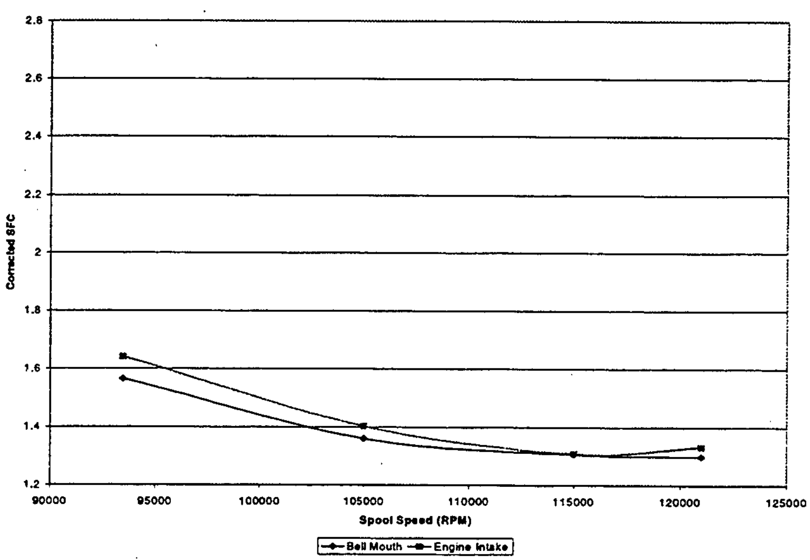

Figure 6b. SFC Comparison; Engine Intake vs. Bellmouth

In Figure 6a it can be seen that the thrust vs. spool speed for the engine with intake was also nearly linear. Comparing these results with the engine with bellmouth showed a slight decrease in thrust for the spool speeds tested. The reduction in thrust was approximately 3% for the range of speeds tested. From Figure 6b, the engine intake SFC vs spool speed had a similar behavior to the engine with bellmouth configuration, with the greatest difference in results at about 80% spool speed (95000 RPM). At 100% spool speed, the SFC for the two engine configurations were nearly identical. The SFC for the engine intake increased slightly from 100% to 105%.

3. Baseline Shroud Configuration

Comparing the baseline shroud with the engine intake in Figure 7a, it was noted that the thrust vs. spool speed for both configurations showed a nearly linear relationship throughout the range of speeds tested. From 80% spool speed to 100% spool speed the difference in output between the two configurations converged from 5% to the same value at 100% spool speed. As was expected, the thrust levels were the same for both configurations, indicating that no additional flow was entrained through the baseline shroud. The SFC comparison in Figure 7b showed that the engine intake configuration performed better at all speeds.

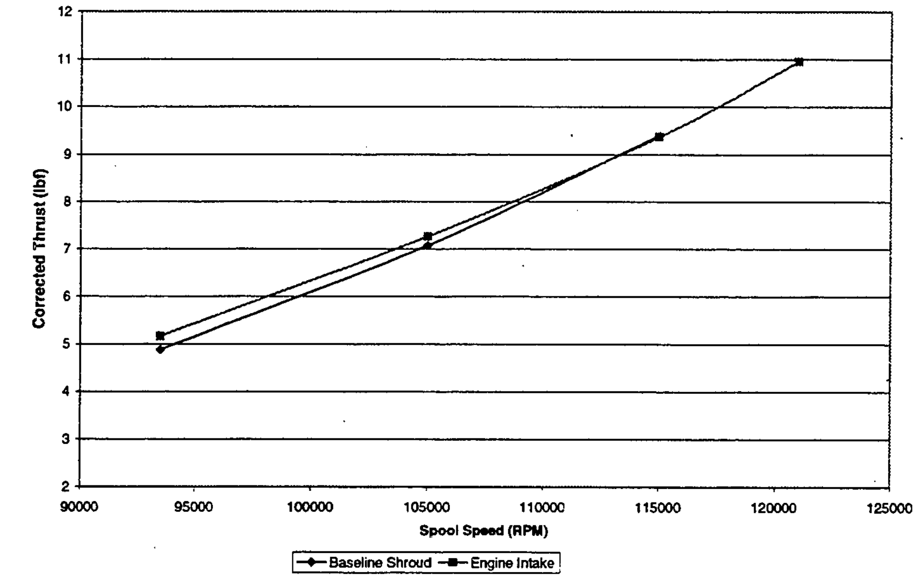

Figure 7a. Thrust Comparison; Baseline Shroud vs. Engine Intake

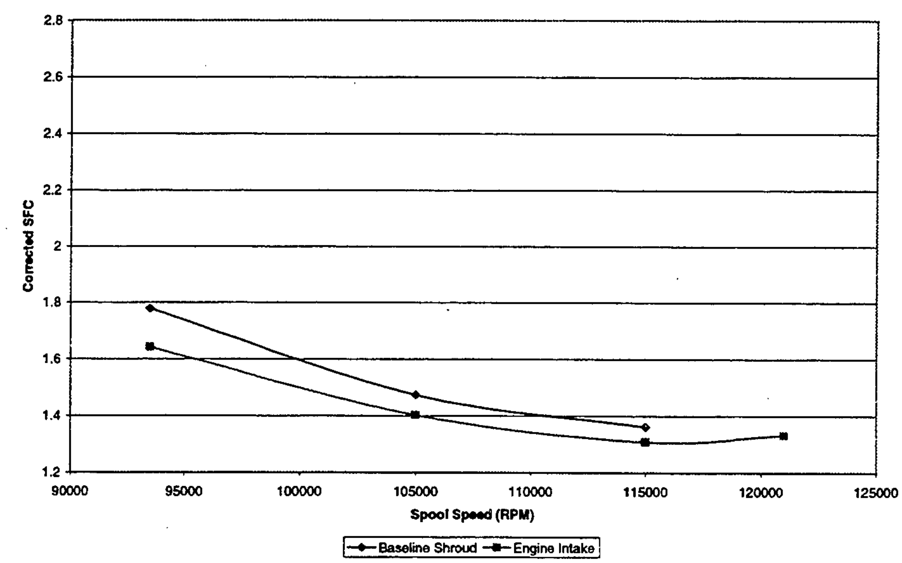

Figure 7b. SFC Comparison; Baseline Shroud vs. Engine Intake

4. Short Shroud Configurations

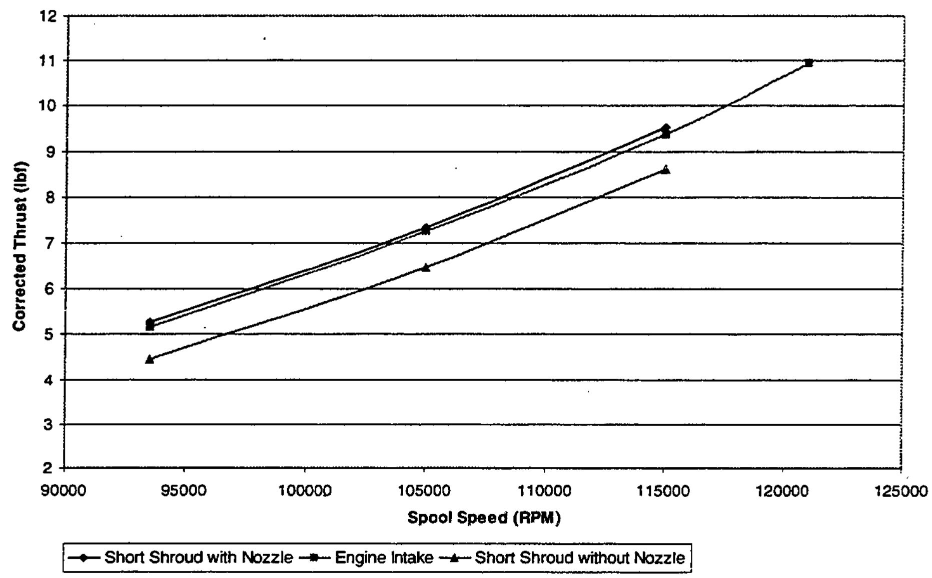

Figure 8a. Thrust Comparison; Short Shroud vs. Engine Intake

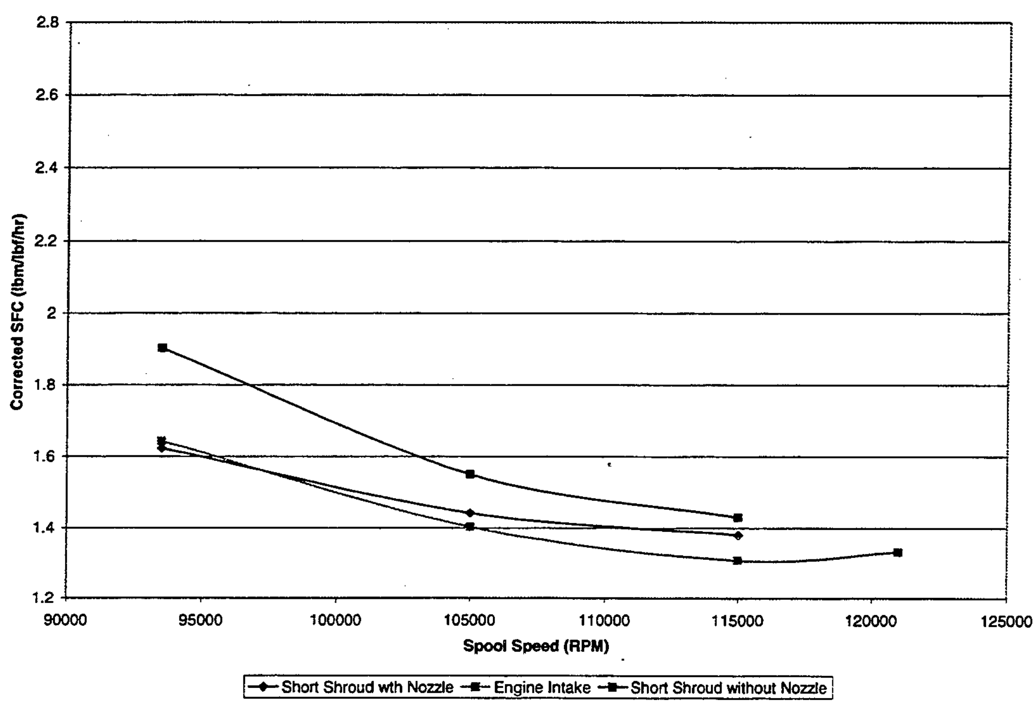

Figure 8b. SFC Comparison; Short Shroud vs. Engine Intake

The thrust output from the short shroud with nozzle, shown in Figure 8a, was slightly above that of the engine intake configuration. The short shroud without nozzle configuration displayed a reduced performance level for all spool speeds tested. The SFC comparison in Figure 8b showed that the engine intake configuration had a better performance than either of the short shroud configurations, especially at higher spool speeds. Comparing the two short shroud configurations showed that the nozzle was beneficial to both the thrust output and the SFC. In Figure 9, the short shroud with nozzle displayed a higher level of secondary flow entrainment, indicated by the lower pressure distribution throughout the shroud. The minimum entrainment pressure recorded on the shroud was 2.65" of water. The short shroud with nozzle produced a sharp increase in pressure at the exit of the shroud due to the presence of the converging nozzle. Similar trends were noted at the reduced spool speeds, the results of which are tabulated in Appendix F.

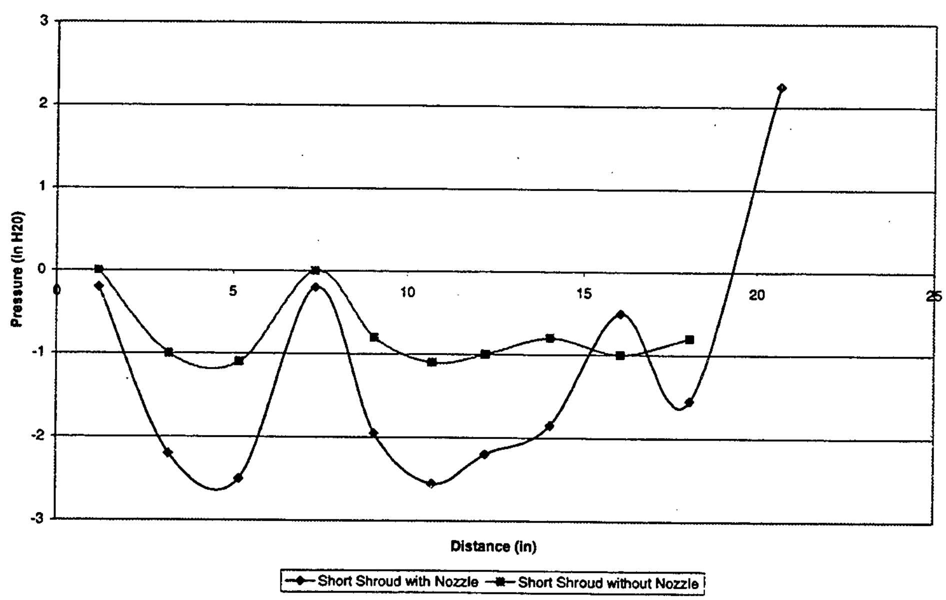

Figure 9. Short Shroud Pressure Distribution at 100% Spool Speed

5. Medium Shroud Configurations

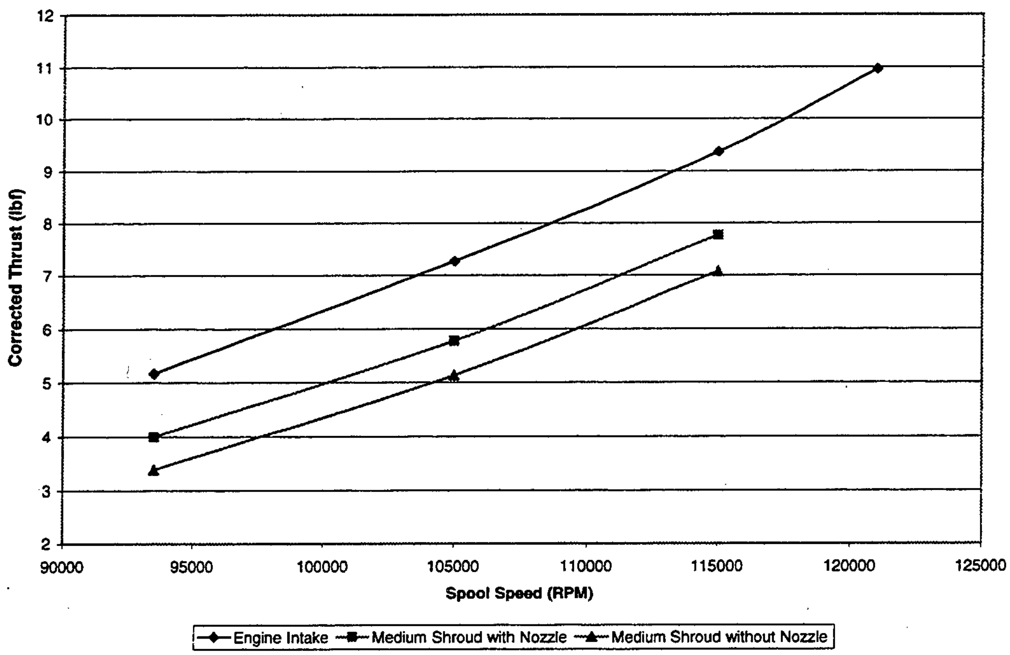

Figure 10a. Thrust Comparison; Medium Shroud with Elliptic Intake

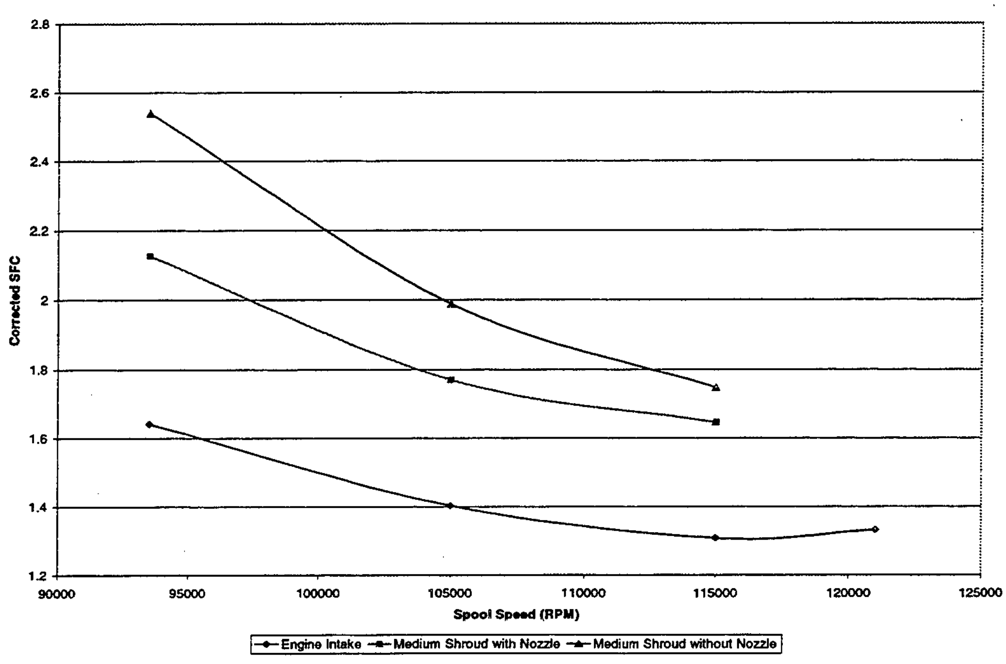

Figure 10b. SFC Comparison; Medium Shroud with Elliptic Intake

The medium shroud with nozzle degraded the thrust output by 16% over the speed range, while the medium shroud without nozzle degraded the thrust by 26% (Fig. 10a). Similarly the medium shroud increased the SFC by 26% with the nozzle on and by 34% without the nozzle (Fig 10b). The shroud pressure distributions were similar to those measured on the short shroud; however, the minimum entrainment pressure was reduced below 3" of water (Fig. 11). At 100% spool speed the exhaust gas temperature was measured at 585^0 F with the nozzle, and 646^0 F without the nozzle (Appendix D).

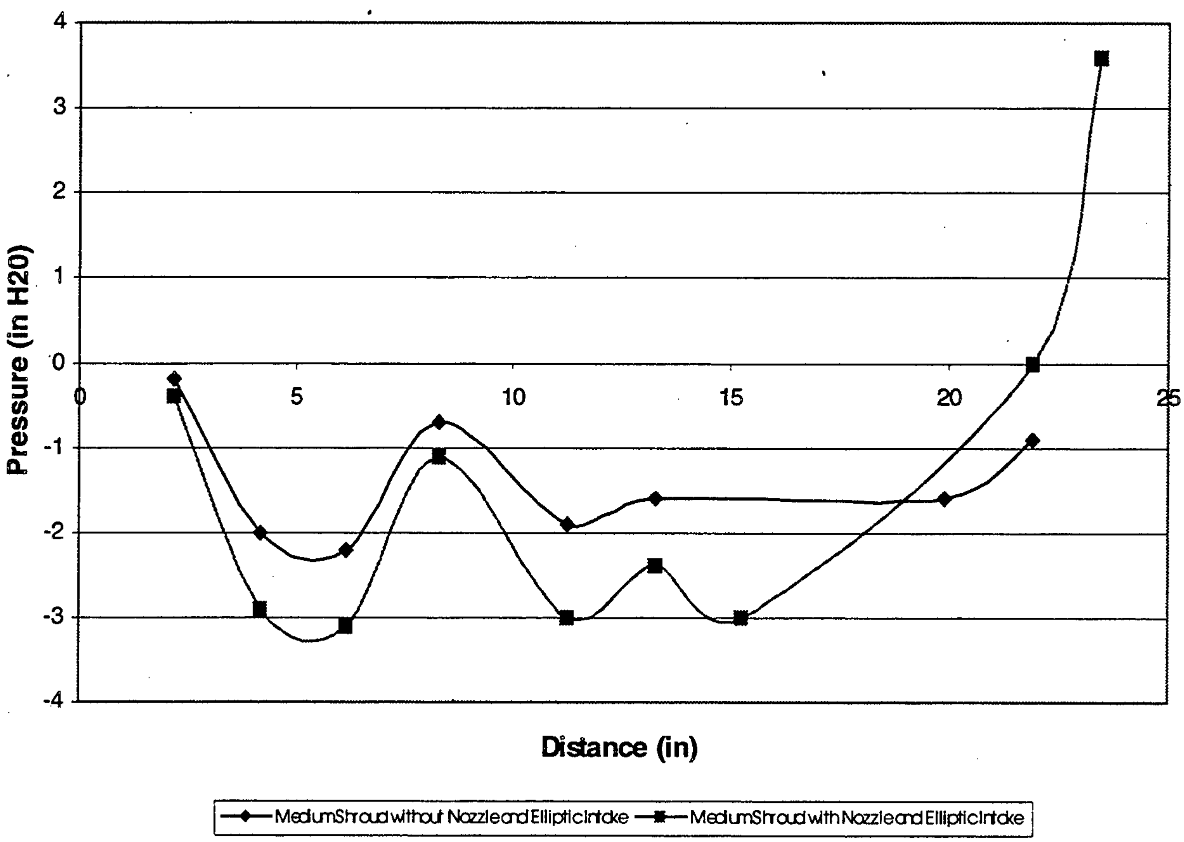

Figure 11. Medium Shroud with Elliptic Intake Pressure Distribution at 100% Spool Speed

Long Shroud Configurations

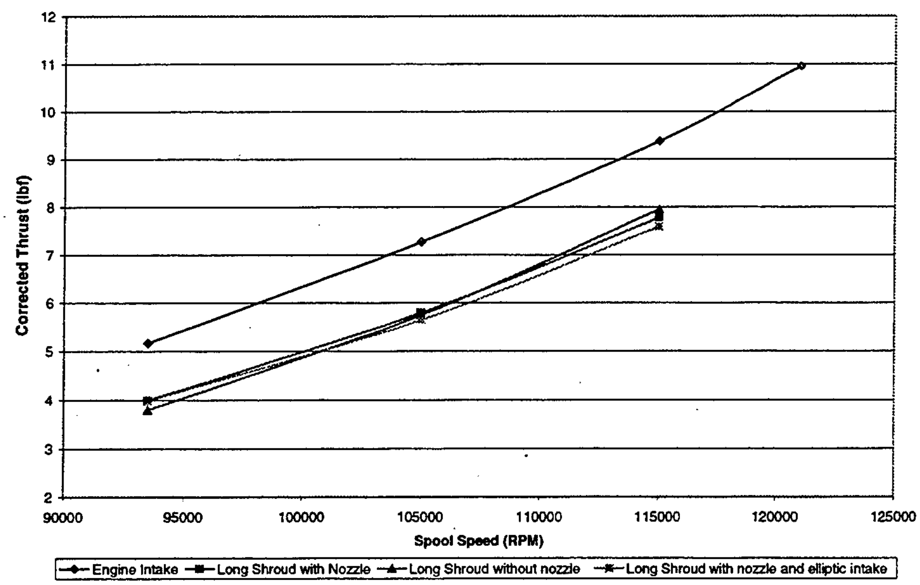

Figure 12a. Thrust Comparison; Long Shroud

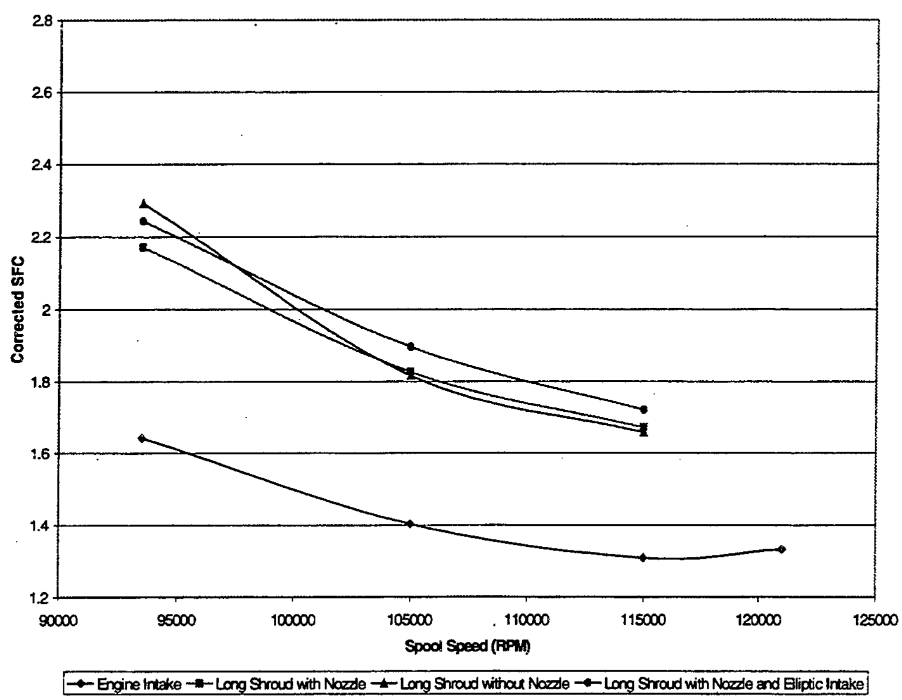

Figure 12b. SFC Comparison; Long Shroud

The long shroud with nozzle degraded the thrust output by 15% over the speed range, while the long shroud without nozzle degraded the thrust by 16% (Fig.12a). Similarly the long shroud increased the SFC by 26% with the nozzle on and by 28% without the nozzle (Fig. 12b). The shroud pressure distributions were similar to those measured on the short shroud; however, the minimum entrainment pressure was reduced below 3.5" of water (Fig.13). Of note were the high positive pressure at the two final pressure taps on the nozzle. This indicated that the final duct was at a significantly higher pressure than atmospheric pressure, which limited the amount of secondary flow entrainment. At 100% spool speed the exhaust gas temperature was measured at 580^0 F with the nozzle on (Appendix D).

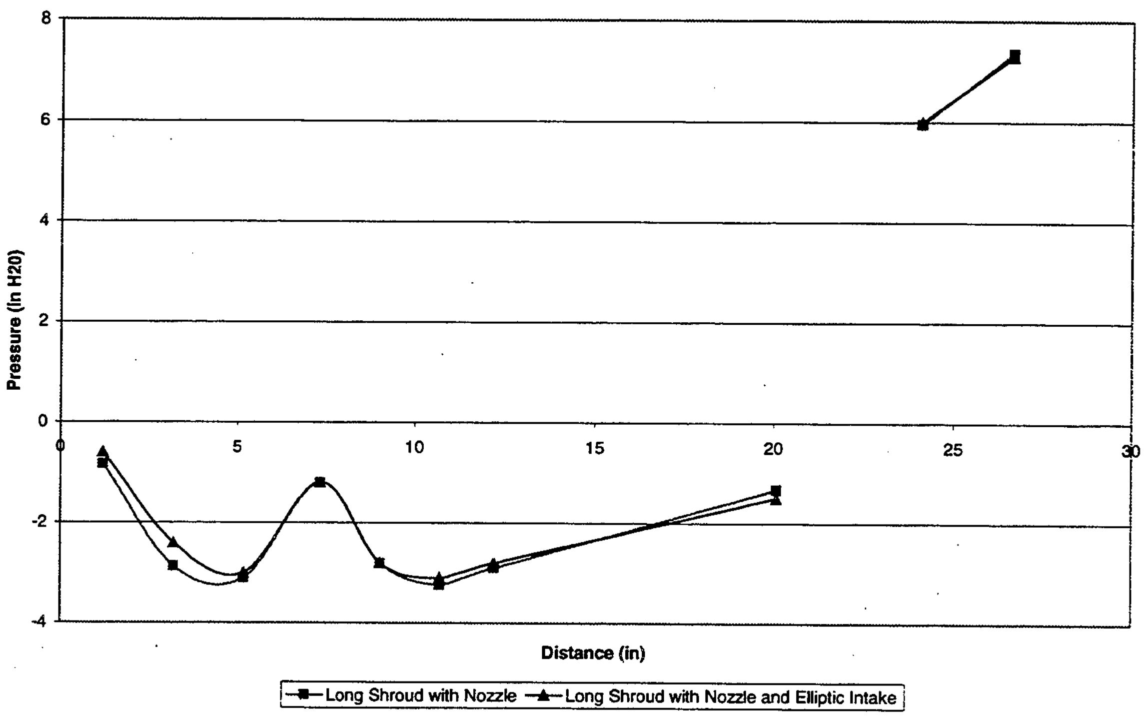

Figure 13. Long Shroud Pressure Distribution, 100% Spool Speed

THIS PAGE INTENTIONALLY LEFT BLANK

D. SUMMARY AND COMPARISON OF RESULTS

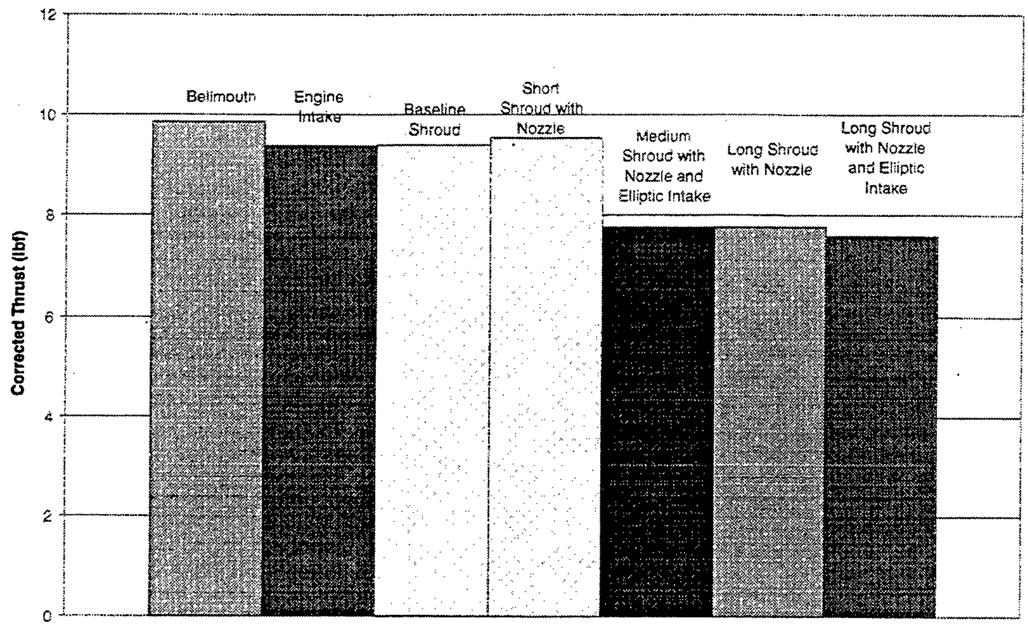

Figure 14a. Thrust Comparison at 100% Spool Speed

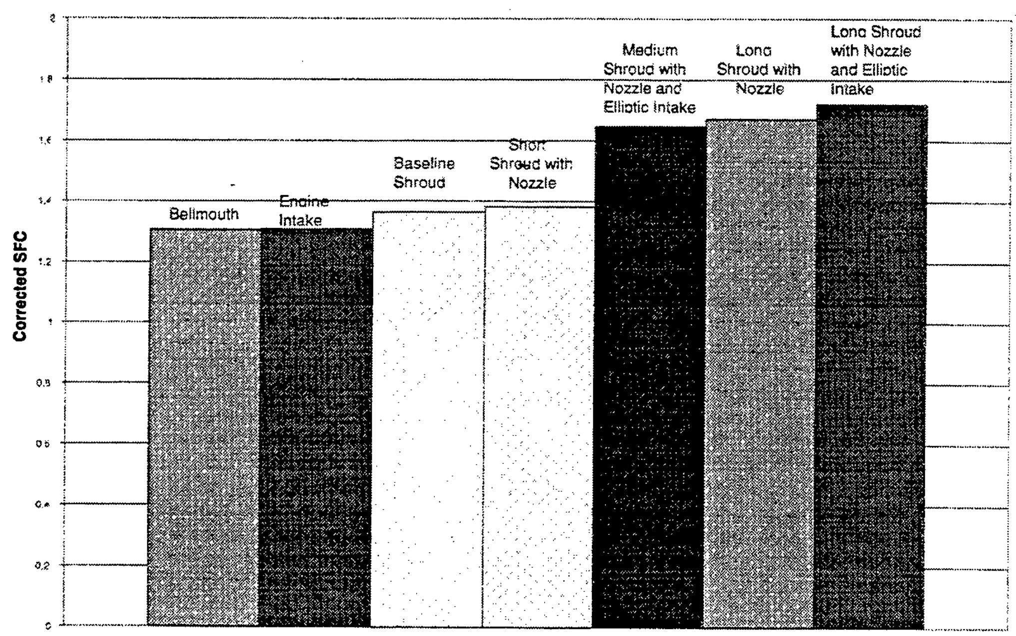

Figure 14b. SFC Comparison at 100% Spool Speed

As we can see from the thrust comparison (Fig. 14a), at 100% spool speed the best configurations were the bellmouth and short shroud with nozzle. The engine intake and the baseline shroud showed a small decrease in thrust output from the previous two configurations. The remaining configurations showed a marked decrease in performance. For the SFC comparison (Fig. 14b), the bellmouth and the engine intake provided the best results, and were nearly identical. The performance of the baseline shroud, and the short shroud with nozzle, were slightly higher than the engine with intake; however, the short shroud performance was acceptable over the full operating range.

The entrainment pressures on the shroud are shown plotted for 100% spool speed for the short, medium, and long shrouds in Figure 15. The distance on the horizontal axis was taken from the front flange of the shroud and not from the front of elliptic intake. Overall, the shape of the pressure distribution over the front of the shroud remained unchanged; however, the medium shroud experienced the minimum suction pressure. As the duct length increased, the final positive pressure in the nozzle increased. This positive pressure was probably a significant factor in controlling the overall entrainment rate into the shroud.

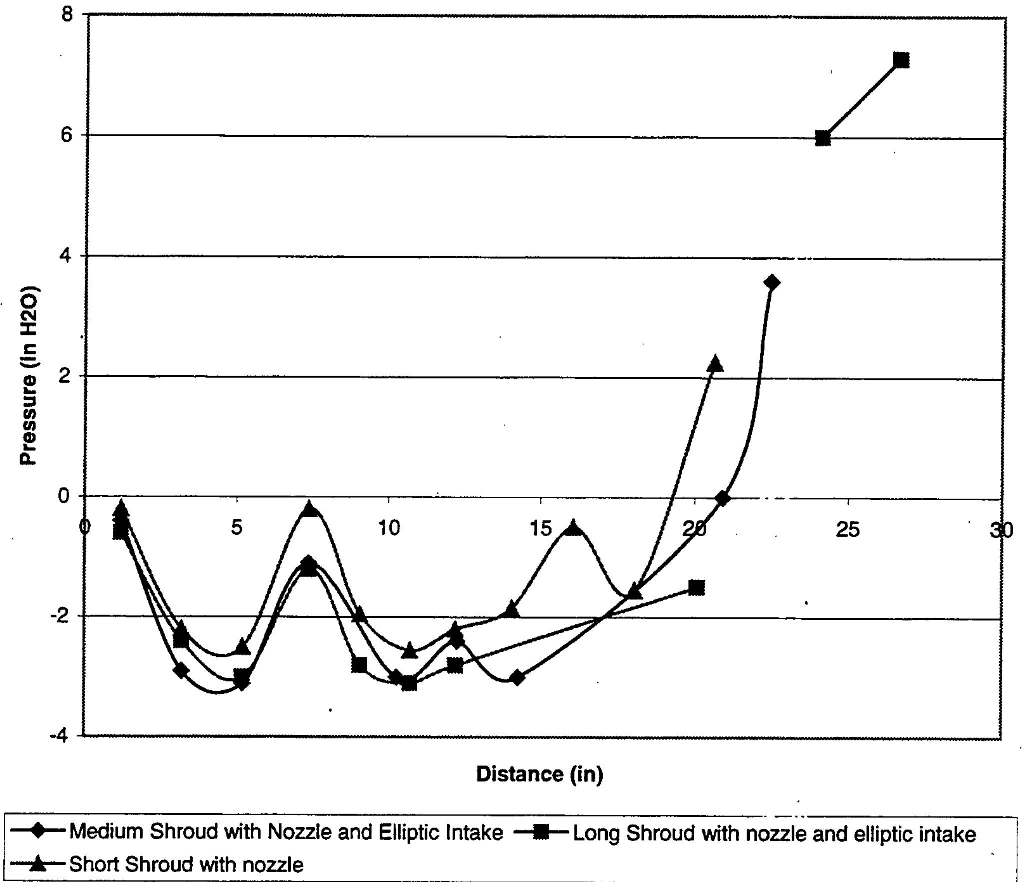

Figure 15. Long, Medium, Short Shroud Pressure Distributions

THIS PAGE INTENTIONALLY LEFT BLANK

III. CONCLUSIONS AND RECOMMENDATIONS

A. CONCLUSIONS

The investigation of initial shroud configurations toward the development of a turbo-ramjet engine, formed the motivation for this thesis. It was found that the shroud configuration significantly affected the performance. The short shroud with nozzle provided better performance than the clean engine. This performance increase was observed to be more significant at lower engine speeds. At 80% spool speed, an increase of approximately 2% thrust was noted, which decreased as spool speed increased. The SFC was approximately 5% better than the clean engine, for all speeds tested.

It was found that for the static conditions, the elliptic intake did not affect the results for the two configurations tested (medium and long shrouds). The medium length shroud had the minimum suction pressure along the length of the duct, which should have indicated maximum secondary flow entrainment. The long shroud gave the maximum positive pressure at the nozzle exit, since, it is suggested, the engine exhaust had diverged enough to significantly affect the shroud nozzle flow.

B. RECOMMENDATIONS

The effects of forward flight should be investigated by placing the engine and shroud in a free jet facility and repeating the abovementioned tests.

A supersonic intake needs to be designed for the combined cycle engine. A design Mach number needs to be chosen and an off-design analysis performed at other flight Mach number's. A ramjet combustion chamber (afterburner) needs to be designed and tested for the shroud assembly to fully test a turbo-ramjet combination.

THIS PAGE INTENTIONALLY LEFT BLANK

APPENDIX A. DRAWINGS

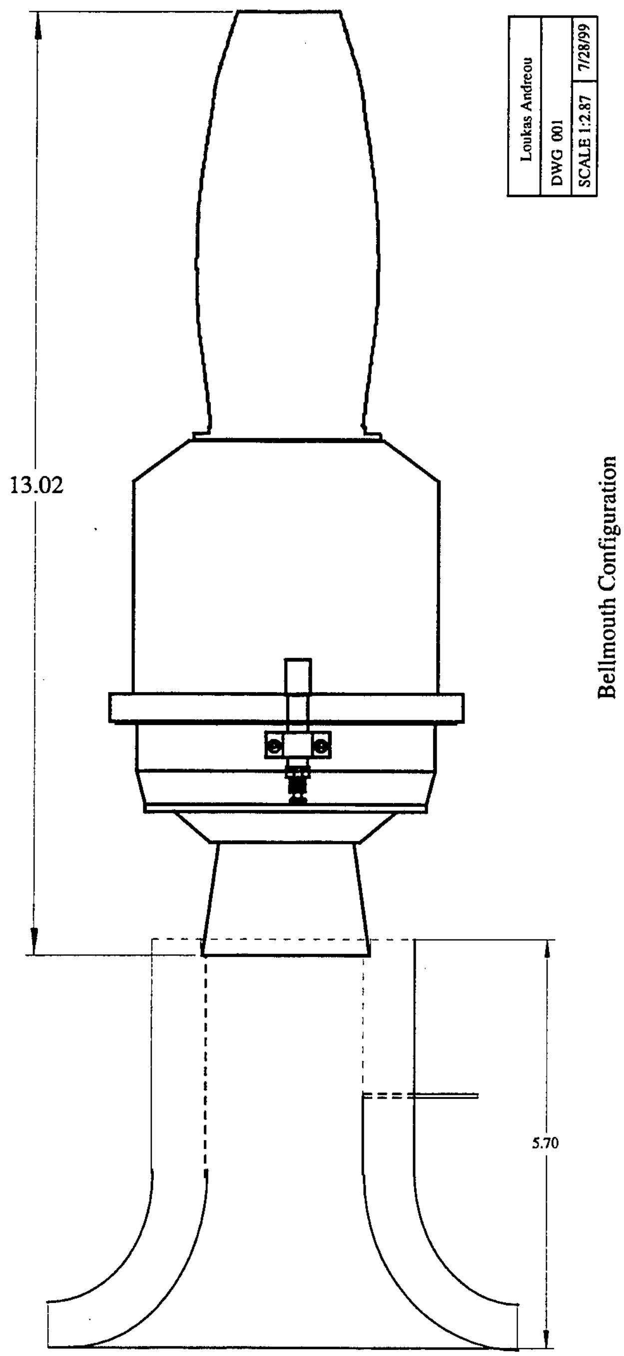

Figure A-1. Bellmouth Configuration

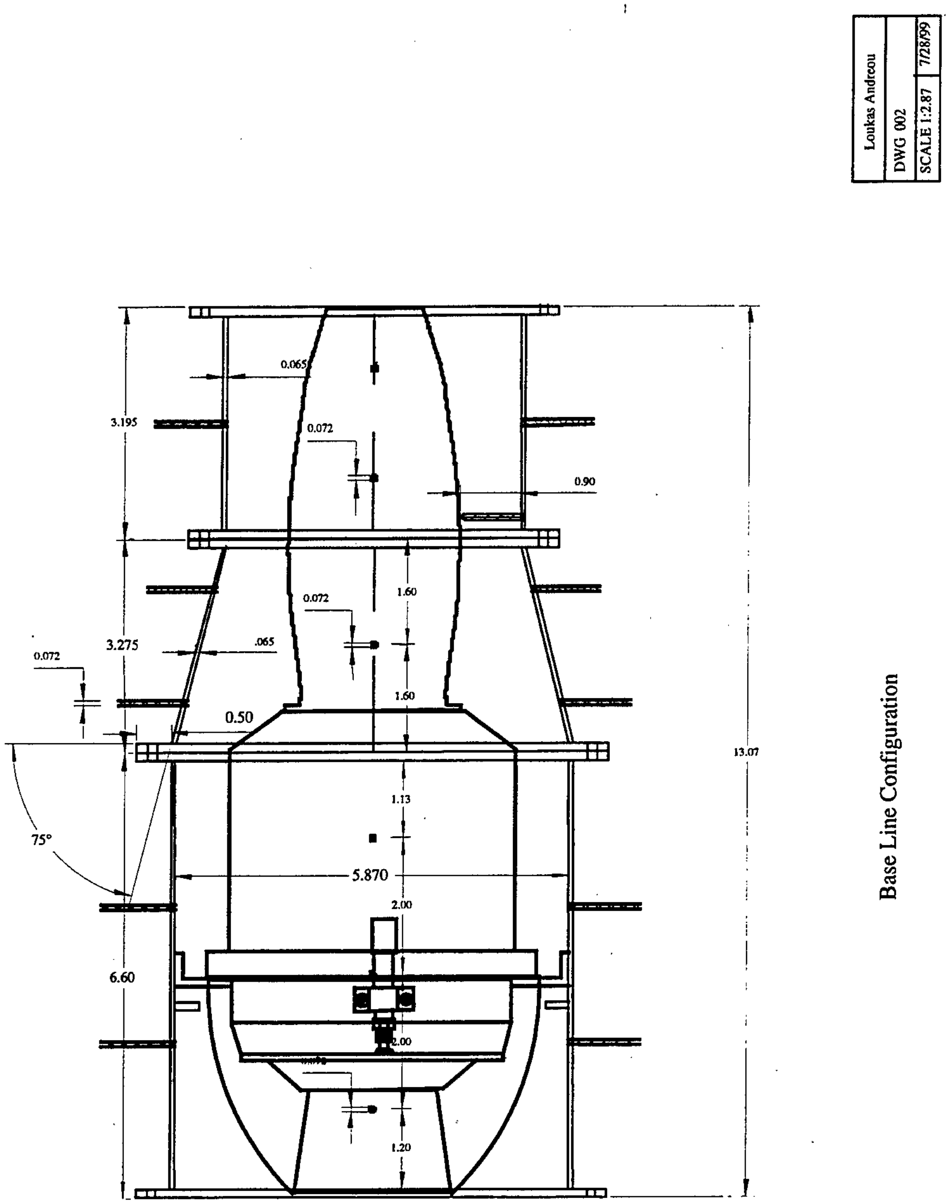

Figure A-2. Baseline Shroud Configuration and Engine with Flight Intake

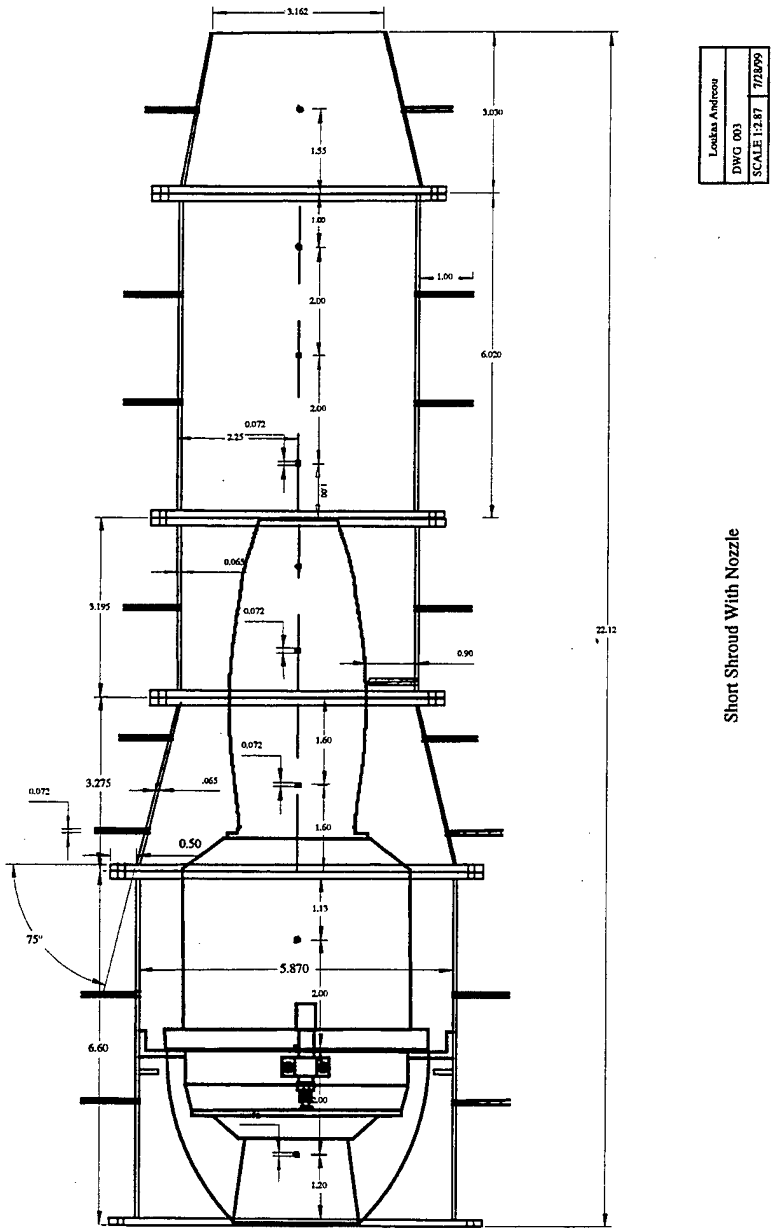

Figure A-3. Short Shroud With Nozzle and Elliptic Intake Configuration

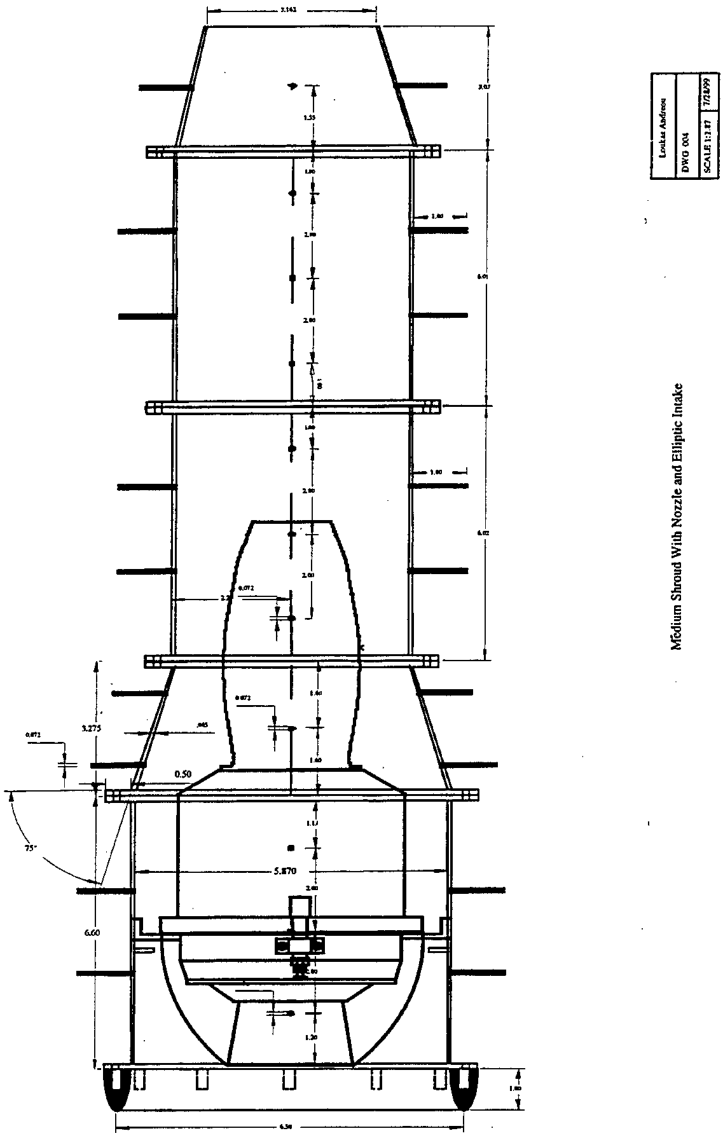

Figure A-4. Medium Shroud With Nozzle and Elliptic Intake Configuration

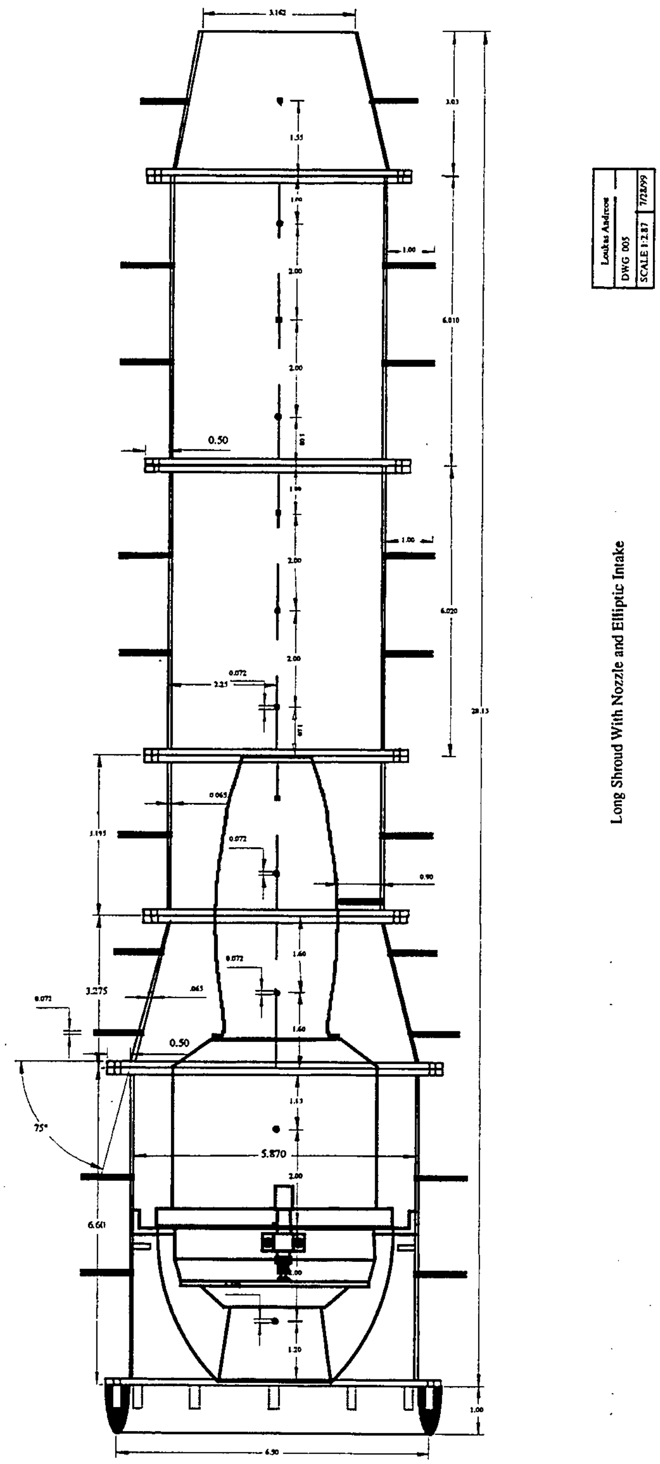

Figure A-5. Long Shroud With Nozzle and Elliptic Intake Configuration

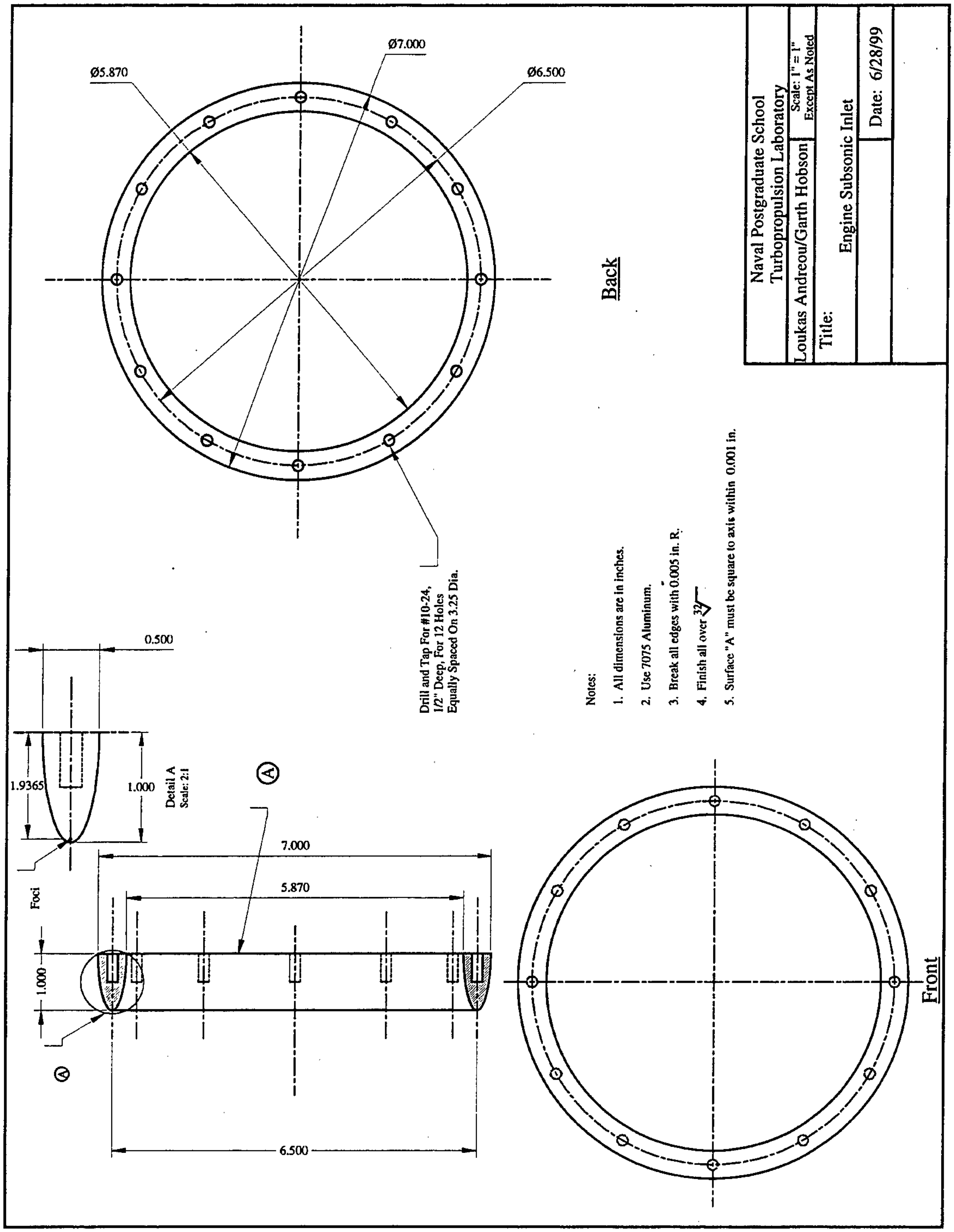

Figure A-6. Elliptic Inlet Design

APPENDIX B. THRUST AND SFC PLOTS

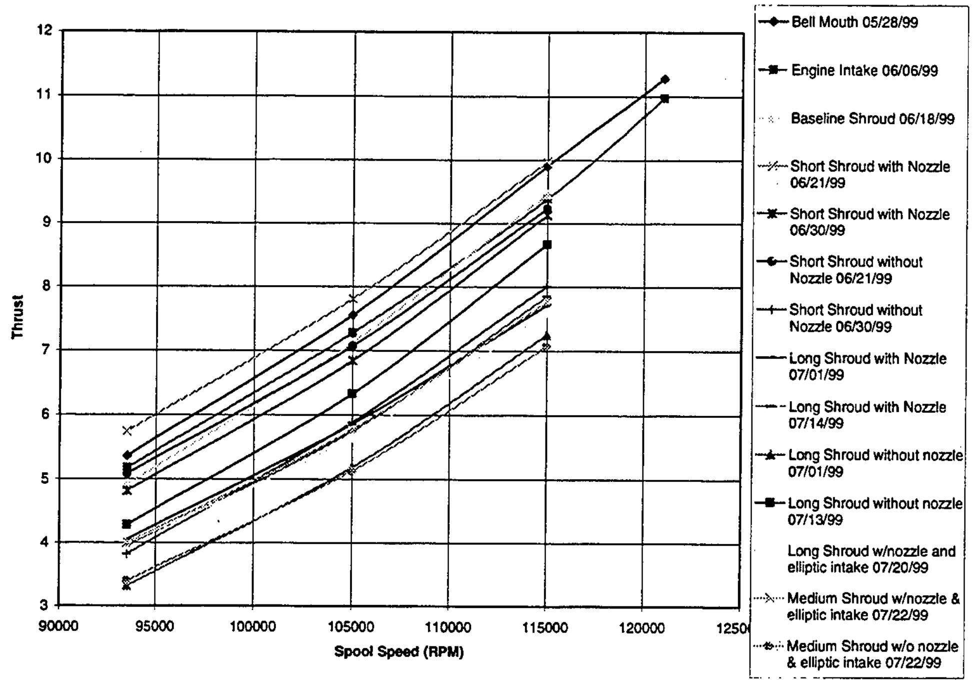

Figure B-1. Thrust Comparison

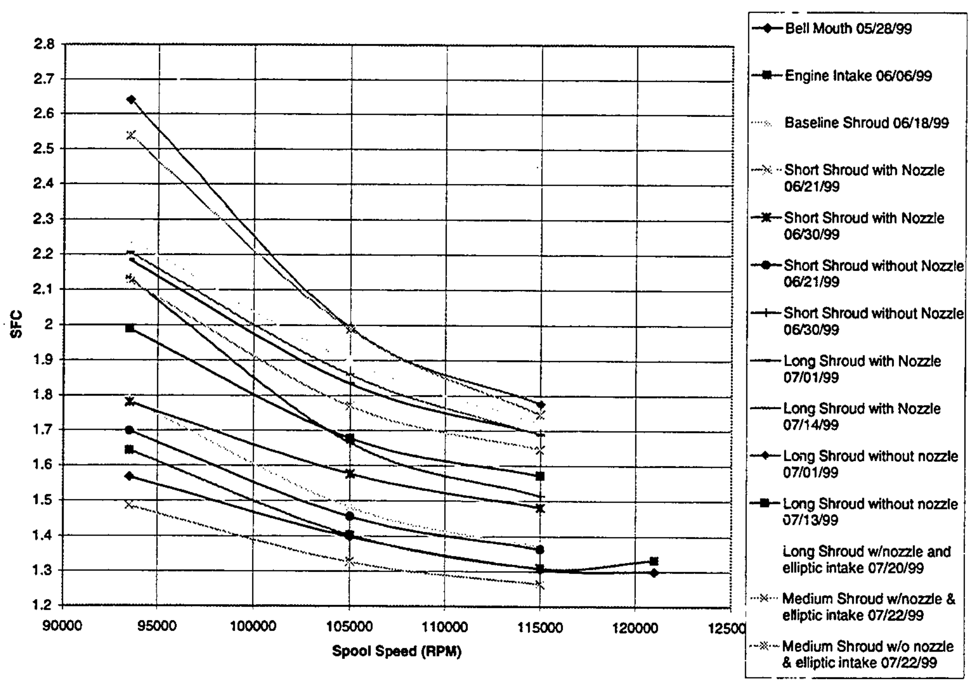

Figure B-2. SFC Comparison

THIS PAGE INTENTIONALLY LEFT BLANK

APPENDIX C. SOPHIA J450 THRUST RESULTS

SOPHIA J450 TEST DATA (BELLMOUTH)
DATE: 28 MAY 1999
Pamb: 1019 mbar
Temperature: 61^{0}F

105% spool speed				
Run	**Thrust (lbf)**	**Fuel flow(m_f) (lbm/sec)**	**SFC (lbm/lb/hr)**	**Mass flow (m_a) (lbm/sec)**
1	11.2601	-	-	0.29335
2	11.3566	0.004045	1.28225	0.30121
3	11.2095	0.004102	1.31738	0.29460
Average	11.2754	0.004073	1.29981	0.29638

100% spool speed				
Run	**Thrust (lbf)**	**Fuel flow(m_f) (lbm/sec)**	**SFC (lbm/lb/hr)**	**Mass flow (m_a) (lbm/sec)**
1	9.8336	-	-	0.28554
2	9.9389	0.003572	1.29382	0.28134
3	9.9435	0.003651	1.32182	0.27754
Average	9.9053	0.003611	1.30782	0.28147

90% spool speed				
Run	**Thrust (lbf)**	**Fuel flow(m_f) (lbm/sec)**	**SFC (lbm/lb/hr)**	**Mass flow (m_a) (lbm/sec)**
1	7.5478	-	-	0.24688
2	7.5623	0.002931	1.39529	0.25102
3	7.5586	0.002943	1.40168	0.24997
Average	7.5562	0.002937	1.39848	0.24929

80% spool speed				
Run	**Thrust (lbf)**	**Fuel flow(m_f) (lbm/sec)**	**SFC (lbm/lb/hr)**	**Mass flow (m_a) (lbm/sec)**
1	5.3684	-	-	0.20334
2	5.3546	0.002354	1.58264	0.20633
3	5.3585	0.002313	1.55394	0.20205
Average	5.3605	0.002333	1.56829	0.20390

SOPHIA J450 TEST DATA (ENGINE INTAKE)

DATE: 6 JUN 1999
Pamb: 1015 mbar
Temperature: 60^0 F

	105% spool speed		
Run	**Thrust (lbf)**	**Fuel flow(m_f) (lbm/sec)**	**SFC (lbm/lb/hr)**
1	10.9200	-	-
2	11.0081	0.004045	1.32284
3	10.9918	0.004102	1.34347
Average	10.9733	0.004073	1.33315

	100% spool speed		
Run	**Thrust (lbf)**	**Fuel flow(m_f) (lbm/sec)**	**SFC (lbm/lb/hr)**
1	9.4003	-	-
2	9.3900	0.003310	1.26900
3	9.3726	0.003515	1.35010
Average	9.3876	0.003412	1.30955

	90% spool speed		
Run	**Thrust (lbf)**	**Fuel flow(m_f) (lbm/sec)**	**SFC (lbm/lb/hr)**
1	7.2607	-	-
2	7.2770	0.002848	1.40893
3	7.2996	0.002837	1.39914
Average	7.2791	0.002842	1.40403

	80% spool speed		
Run	**Thrust (lbf)**	**Fuel flow(m_f) (lbm/sec)**	**SFC (lbm/lb/hr)**
1	5.1185	-	-
2	5.1925	0.002423	1.67988
3	5.2093	0.002326	1.60743
Average	5.1734	0.002374	1.64365

SOPHIA J450 TEST DATA (BASELINE SHROUD)
DATE: 6 JUN 1999
Pamb: 1020 mbar
Temperature: 65^0 F

	100% spool speed		
Run	**Thrust (lbf)**	**Fuel flow(m_f) (lbm/sec)**	**SFC (lbm/lb/hr)**
1	9.4669	-	-
2	9.4480	0.003560	1.35647
3	9.4659	0.003632	1.38129
Average	9.4602	0.003596	1.36888

	90% spool speed		
Run	**Thrust (lbf)**	**Fuel flow(m_f) (lbm/sec)**	**SFC (lbm/lb/hr)**
1	7.1259	-	-
2	7.1088	0.002910	1.47366
3	7.1455	0.002958	1.49028
Average	7.1267	0.002934	1.48197

	80% spool speed		
Run	**Thrust (lbf)**	**Fuel flow(m_f) (lbm/sec)**	**SFC (lbm/lb/hr)**
1	4.8566	-	-
2	4.9298	0.002482	1.81248
3	4.9379	0.002419	1.76358
Average	4.9081	0.002450	1.78803

SOPHIA J450 TEST DATA (SHORT SHROUD WITH NOZZLE)
DATE: 21 JUN 1999
Pamb: 1014 mbar
Temperature: 63^0 F

	100% spool speed		
Run	**Thrust (lbf)**	**Fuel flow(m_f) (lbm/sec)**	**SFC (lbm/lb/hr)**
1	9.9927	-	-
2	9.9645	0.003496	1.26304
3	9.9603	0.003499	1.26466
Average	9.9725	0.003497	1.26385

	90% spool speed		
Run	**Thrust (lbf)**	**Fuel flow(m_f) (lbm/sec)**	**SFC (lbm/lb/hr)**
1	7.7831	-	-
2	7.8190	0.002861	1.31725
3	7.8287	0.002904	1.33539
Average	7.8102	0.002882	1.32632

	80% spool speed		
Run	**Thrust (lbf)**	**Fuel flow(m_f) (lbm/sec)**	**SFC (lbm/lb/hr)**
1	5.7314	-	-
2	5.7427	0.002355	1.47630
3	5.7506	0.002389	1.49556
Average	5.7415	0.002372	1.48593

SOPHIA J450 TEST DATA (SHORT SHROUD WITHOUT NOZZLE)
DATE: 21 JUN 1999
Pamb: 1014 mbar
Temperature: 63^0 F

	100% spool speed		
Run	**Thrust (lbf)**	**Fuel flow(m_f) (lbm/sec)**	**SFC (lbm/lb/hr)**
1	9.3009	-	-
2	9.1862	0.003494	1.36927
3	9.2171	0.003507	1.36975
Average	9.2347	0.003500	1.36951

	90% spool speed		
Run	**Thrust (lbf)**	**Fuel flow(m_f) (lbm/sec)**	**SFC (lbm/lb/hr)**
1	7.0036	-	-
2	7.0826	0.002868	1.45789
3	7.1287	0.002875	1.45187
Average	7.0716	0.002871	1.45488

	80% spool speed		
Run	**Thrust (lbf)**	**Fuel flow(m_f) (lbm/sec)**	**SFC (lbm/lb/hr)**
1	5.0480	-	-
2	5.0800	0.002405	1.70433
3	5.1096	0.002390	1.68388
Average	5.0792	0.002397	1.69410

SOPHIA J450 TEST DATA (MEDIUM SHROUD WITH NOZZLE AND ELLIPTIC INTAKE)

DATE: 22 JUL 1999
Pamb: 1023 mbar
Temperature: 68^0 F

		100% spool speed	
Run	**Thrust (lbf)**	**Fuel flow(m_f) (lbm/sec)**	**SFC (lbm/lb/hr)**
1	7.8256	-	-
2	7.8435	0.003602	1.6532
3	7.8608	0.003633	1.6638
Average	7.8433	0.003617	1.6601

		90% spool speed	
Run	**Thrust (lbf)**	**Fuel flow(m_f) (lbm/sec)**	**SFC (lbm/lb/hr)**
1	5.8268	-	-
2	5.8271	0.002869	1.7724
3	5.8305	0.002909	1.7961
Average	5.8281	0.002889	1.7845

		80% spool speed	
Run	**Thrust (lbf)**	**Fuel flow(m_f) (lbm/sec)**	**SFC (lbm/lb/hr)**
1	4.0483	-	-
2	4.0337	0.002408	2.1490
3	4.0210	0.002399	2.1478
Average	4.0343	0.002403	2.1443

SOPHIA J450 TEST DATA (MEDIUM SHROUD WITHOUT NOZZLE AND ELLIPTIC INTAKE)

DATE: 22 JUL 1999
Pamb: 1023 mbar
Temperature: 68^0 F

	100% spool speed		
Run	**Thrust (lbf)**	**Fuel flow(m_f) (lbm/sec)**	**SFC (lbm/lb/hr)**
1	7.1450	-	-
2	7.1272	0.003513	1.7744
3	7.1567	0.003476	1.7485
Average	7.1429	0.003494	1.7609

	90% spool speed		
Run	**Thrust (lbf)**	**Fuel flow(m_f) (lbm/sec)**	**SFC (lbm/lb/hr)**
1	5.1844	-	-
2	5.1829	0.002881	2.0011
3	5.1710	0.002888	2.0106
Average	5.1794	0.002884	2.0049

	80% spool speed		
Run	**Thrust (lbf)**	**Fuel flow(m_f) (lbm/sec)**	**SFC (lbm/lb/hr)**
1	3.4076	-	-
2	3.4236	0.002435	2.5604
3	3.4468	0.002438	2.5463
Average	3.4260	0.002436	2.5602

SOPHIA J450 TEST DATA (LONG SHROUD WITH NOZZLE)

DATE: 14 JUL 1999
Pamb: 1016 mbar
Temperature: 72^0 F

	100% spool speed		
Run	**Thrust (lbf)**	**Fuel flow(m_f) (lbm/sec)**	**SFC (lbm/lb/hr)**
1	7.8363	-	-
2	7.8380	0.003664	1.6828
3	7.8760	0.003700	1.6912
Average	7.8501	0.003682	1.6885

	90% spool speed		
Run	**Thrust (lbf)**	**Fuel flow(m_f) (lbm/sec)**	**SFC (lbm/lb/hr)**
1	5.7173	-	-
2	5.7487	0.002960	1.8536
3	5.7705	0.002976	1.8566
Average	5.7455	0.002968	1.8596

	80% spool speed		
Run	**Thrust (lbf)**	**Fuel flow(m_f) (lbm/sec)**	**SFC (lbm/lb/hr)**
1	3.9268	-	-
2	3.9380	0.002393	2.1876
3	3.9838	0.002448	2.2121
Average	3.9495	0.002420	2.2058

SOPHIA J450 TEST DATA (LONG SHROUD WITHOUT NOZZLE)

DATE: 13 JUL 1999
Pamb: 1016 mbar
Temperature: 71^0F

	100% spool speed		
Run	**Thrust (lbf)**	**Fuel flow(m_f) (lbm/sec)**	**SFC (lbm/lb/hr)**
1	8.3445	-	-
2	8.8161	0.003727	1.5218
3	8.8510	0.003845	1.5638
Average	8.6705	0.003786	1.5719

	90% spool speed		
Run	**Thrust (lbf)**	**Fuel flow(m_f) (lbm/sec)**	**SFC (lbm/lb/hr)**
1	6.4536	-	-
2	6.2855	0.002980	1.7067
3	6.2506	0.002923	1.6834
Average	6.3299	0.002951	1.6783

	80% spool speed		
Run	**Thrust (lbf)**	**Fuel flow(m_f) (lbm/sec)**	**SFC (lbm/lb/hr)**
1	4.2299	-	-
2	4.2821	0.002367	1.9899
3	4.3319	0.002367	1.9670
Average	4.2813	0.002367	1.9903

SOPHIA J450 TEST DATA (LONG SHROUD WITH NOZZLE)

DATE: 14 JUL 1999
Pamb: 1016 mbar
Temperature: 70^0 F

	100% spool speed		
Run	**Thrust (lbf)**	**Fuel flow(m_f) (lbm/sec)**	**SFC (lbm/lb/hr)**
1	7.8363	-	-
2	7.8380	0.003664	1.6828
3	7.8760	0.003700	1.6912
Average	7.8501	0.003682	1.6885

	900% spool speed		
Run	**Thrust (lbf)**	**Fuel flow(m_f) (lbm/sec)**	**SFC (lbm/lb/hr)**
1	5.7173	-	-
2	5.7487	0.002960	1.8536
3	5.7705	0.002976	1.8566
Average	5.7455	0.002968	1.8596

	80% spool speed		
Run	**Thrust (lbf)**	**Fuel flow(m_f) (lbm/sec)**	**SFC (lbm/lb/hr)**
1	3.9268	-	-
2	3.9380	0.002393	2.1876
3	3.9838	0.002448	2.2121
Average	3.9495	0.002420	2.2058

SOPHIA J450 TEST DATA (LONG SHROUD WITH NOZZLE AND ELLIPTIC INTAKE)

DATE: 20 JUL 1999
Pamb: 1022 mbar
Temperature: 68^0 F

	100% spool speed		
Run	**Thrust (lbf)**	**Fuel flow(m_f) (lbm/sec)**	**SFC (lbm/lb/hr)**
1	7.6008	-	-
2	7.6624	0.003665	1.7219
3	7.6935	0.003710	1.7360
Average	7.6522	0.003687	1.7345

	90% spool speed		
Run	**Thrust (lbf)**	**Fuel flow(m_f) (lbm/sec)**	**SFC (lbm/lb/hr)**
1	5.6228	-	-
2	5.7614	0.003023	1.8889
3	5.6916	0.003025	1.9133
Average	5.6919	0.003024	1.9126

	80% spool speed		
Run	**Thrust (lbf)**	**Fuel flow(m_f) (lbm/sec)**	**SFC (lbm/lb/hr)**
1	3.9985	-	-
2	4.0238	0.002532	2.2653
3	4.0366	0.002519	2.2465
Average	4.0196	0.002525	2.2614

SOPHIA J450 TEST DATA (MEDIUM SHROUD WITH NOZZLE AND ELLIPTIC INTAKE)

DATE: 22 JUL 1999
Pamb: 1023 mbar
Temperature: 68^0 F

	100% spool speed		
Run	**Thrust (lbf)**	**Fuel flow(m_f) (lbm/sec)**	**SFC (lbm/lb/hr)**
1	7.8256	-	-
2	7.8435	0.003602	1.6532
3	7.8608	0.003633	1.6638
Average	7.8433	0.003617	1.6601

	90% spool speed		
Run	**Thrust (lbf)**	**Fuel flow(m_f) (lbm/sec)**	**SFC (lbm/lb/hr)**
1	5.8268	-	-
2	5.8271	0.002869	1.7724
3	5.8305	0.002909	1.7961
Average	5.8281	0.002889	1.7845

	80% spool speed		
Run	**Thrust (lbf)**	**Fuel flow(m_f) (lbm/sec)**	**SFC (lbm/lb/hr)**
1	4.0483	-	-
2	4.0337	0.002408	2.1490
3	4.0210	0.002399	2.1478
Average	4.0343	0.002403	2.1443

SOPHIA J450 TEST DATA (MEDIUM SHROUD WITHOUT NOZZLE AND ELLIPTIC INTAKE)

DATE: 22 JUL 1999
Pamb: 1023 mbar
Temperature: 68^0 F

		100% spool speed	
Run	**Thrust (lbf)**	**Fuel flow(m_f) (lbm/sec)**	**SFC (lbm/lb/hr)**
1	7.1450	-	-
2	7.1272	0.003513	1.7744
3	7.1567	0.003476	1.7485
Average	7.1429	0.003494	1.7609

		90% spool speed	
Run	**Thrust (lbf)**	**Fuel flow(m_f) (lbm/sec)**	**SFC (lbm/lb/hr)**
1	5.1844	-	-
2	5.1829	0.002881	2.0011
3	5.1710	0.002888	2.0106
Average	5.1794	0.002884	2.0049

		80% spool speed	
Run	**Thrust (lbf)**	**Fuel flow(m_f) (lbm/sec)**	**SFC (lbm/lb/hr)**
1	3.4076	-	-
2	3.4236	0.002435	2.5604
3	3.4468	0.002438	2.5463
Average	3.4260	0.002436	2.5602

THIS PAGE INTENTIONALLY LEFT BLANK

APPENDIX D. EXHAUST GAS TEMPERATURE TABLE

SPOOL SPEED	LONG SHROUD WITH NOZZLE AND ELLIPTIC INTAKE [^{0} F]	MEDIUM NOZZLE WITH NOZZLE AND ELLIPTIC INTAKE [^{0} F]	MEDIUM NOZZLE WITHOUT NOZZLE AND ELLIPTIC INTAKE [^{0} F]
100%	580	585	646
90%	538	538	620
80%	516	524	581

THIS PAGE INTENTIONALLY LEFT BLANK

APPENDIX E. PRESSURE MEASUREMENTS

SOPHIA J450 TEST DATA (SHORT SHROUD WITH NOZZLE)

DATE: 24 JUN 1999

Pamb: 1017 mbar

Temperature: 65^0 F

100% spool speed

ENGINE PORT	ZOC PORT	ZOC PRESSURE("H_2O)	MANOMETER ("H_2O)
A	1	+0.05520	+0.1
B	2	-0.48024	-1.3
C	3	-0.63880	-1.5
D	4	-0.37950	+0.8
E	5	-0.23046	-0.9
F	6	-0.59726	-1.6
G			-1.2
H			-0.9
I			-0.5
J	7	-0.19458	-0.5
K	8	+0.10791	+3.4

90% spool speed

ENGINE PORT	ZOC PORT	ZOC PRESSURE("H_2O)	MANOMETER ("H_2O)
A	1	-0.29269	+0.8
B	2	-0.06403	-1.0
C	3	-0.44201	-1.1
D	4	-0.04968	+0.6
E	5	-0.55103	-0.8
F	6	-0.50121	-1.3
G			-1.0
H			-0.8
I			-0.5
J	7	-0.20424	-0.5
K	8	+0.21528	+3.0

80% spool speed

ENGINE PORT	ZOC PORT	ZOC PRESSURE("H_2O)	MANOMETER ("H_2O)
A	1	-0.17940	+0.6
B	2	-0.07134	-0.65
C	3	-0.41965	-0.8
D	4	-0.17388	+0.6
E	5	-0.50701	-0.5
F	6	-0.31740	-0.8
G			-0.65
H			-0.4
I			-0.2
J	7	-0.22038	-0.2
K	8	-0.16008	+1.6

SOPHIA J450 TEST DATA (SHORT SHROUD WITHOUT NOZZLE)
DATE: 24 JUN 1999
Pamb: 1017 mbar
Temperature: 65^0 F

100% spool speed

ENGINE PORT	ZOC PORT	ZOC PRESSURE("H_2O)	MANOMETER ("H_2O)
A	1	+0.32154	+0.0
B	2	-0.15000	-1.0
C	3	-0.39578	-1.1
D	4	-0.39468	+0.0
E	5	-0.23046	-0.8
F	6	-0.31284	-1.1
G			-1.0
H			-0.8
I			-0.8
J	7	+0.00897	-1.0
K	8	-0.08556	-0.8

90% spool speed

ENGINE PORT	ZOC PORT	ZOC PRESSURE("H_2O)	MANOMETER ("H_2O)
A	1	-0.16339	-0.4
B	2	-0.07079	-1.1
C	3	-0.35134	-1.2
D	4	+0.0276	-0.4
E	5	-0.38860	-1.1
F	6	+0.07866	-1.2
G			-1.2
H			-1.1
I			-1.1
J	7	-0.07465	-1.1
K	8	-0.25944	-1.1

80% spool speed

ENGINE PORT	ZOC PORT	ZOC PRESSURE("H_2O)	MANOMETER ("H_2O)
A	1	-0.12171	-0.2
B	2	-0.11592	-0.7
C	3	-0.02070	-0.8
D	4	+0.13386	-0.2
E	5	-0.15180	-0.6
F	6	-0.12889	-0.8
G			-0.8
H			-0.8
I			-0.7
J	7	-0.04471	-0.7
K	8	-0.03174	+0.0

SOPHIA J450 TEST DATA (MEDIUM SHROUD WITH NOZZLE AND ELLIPTIC INTAKE)

DATE: 22 JUL 1999

Pamb: 1023 mbar

Temperature: 68^0 F

	100% spool speed	**90% spool speed**	**80% spool speed**
ENGINE PORT	Manometer (“H_2O)	Manometer (“H_2O)	Manometer (“H_2O)
A	-0.4	-0.3	-0.2
B	-2.9	-2.3	-1.7
C	-3.1	-2.5	-1.9
D	-1.1	-0.9	-0.6
E	-3.0	-2.3	-1.5
F	-2.4	-2.0	-1.4
G	-3.0	-2.3	-1.7
H	-0.0	-0.2	-0.5
I	+3.6	+2.5	+3.0

SOPHIA J450 TEST DATA (MEDIUM SHROUD WITH NOZZLE AND ELLIPTIC INTAKE)

DATE: 22 JUL 1999

Pamb: 1023 mbar

Temperature: 68^0 F

	100% spool speed	**90% spool speed**	**80% spool speed**
ENGINE PORT	Manometer (“H_2O)	Manometer (“H_2O)	Manometer (“H_2O)
A	-0.4	-0.3	-0.2
B	-2.9	-2.3	-1.7
C	-3.1	-2.5	-1.9
D	-1.1	-0.9	-0.6
E	-3.0	-2.3	-1.5
F	-2.4	-2.0	-1.4
G	-3.0	-2.3	-1.7
H	-0.0	-0.2	-0.5
I	+3.6	+2.5	+3.0

SOPHIA J450 TEST DATA (MEDIUM SHROUD WITHOUT NOZZLE AND ELLIPTIC INTAKE)

DATE: 22 JUL 1999

Pamb: 1023 mbar

Temperature: 68^0 F

	100% spool speed	**90% spool speed**	**80% spool speed**
ENGINE PORT	Manometer ("H_2O)	Manometer ("H_2O)	Manometer ("H_2O)
A	-0.2	-0.4	-0.2
B	-2.0	-3.0	-3.4
C	-2.2	-3.1	-3.6
D	-0.7	-1.1	-1.2
E	-1.9	-2.8	-3.4
F	-1.6	-2.4	-2.8
G	-1.6	-2.4	-2.8
H	-0.9	-1.3	-1.4

SOPHIA J450 TEST DATA (LONG SHROUD WITH NOZZLE)
DATE: 01 JUL 1999
Pamb: 1014 mbar
Temperature: 70^0 F

		100% spool speed	
ENGINE PORT	ZOC PORT	ZOC PRESSURE("H_2O)	MANOMETER ("H_2O)
A	1	-0.02810	-0.7
B	2	-0.00648	-2.7
C	3	-0.04469	-3.0
D	4	-0.00523	-1.0
E	5	-0.02847	-2.6
F	6	-0.03329	-3.0
G			-2.7
H			-1.5
I			
J	7	0.03255	6.2
K	8	0.05816	7.4

		90% spool speed	
ENGINE PORT	ZOC PORT	ZOC PRESSURE("H_2O)	MANOMETER ("H_2O)
A	1	-0.0043	-1.2
B	2	-0.03284	-5.4
C	3	-0.01282	-5.6
D	4	-0.00892	-2.6
E	5	0.00792	-5.2
F	6	0.00449	-5.9
G			-5.3
H			-4.2
I			
J	7	0.02283	-2.7
K	8	0.0677	-0.7999

		80% spool speed	
ENGINE PORT	ZOC PORT	ZOC PRESSURE("H_2O)	MANOMETER ("H_2O)
A	1	-0.0279	-1.0
B	2	-0.03329	-3.7
C	3	0.00921	-4.0
D	4	-0.01281	-1.7
E	5	-0.01100	-3.5
F	6	-0.02060	-4.2
G			-3.7
H			-3.0
I			
J	7	0.01250	-2.2
K	8	0.00630	-0.7

SOPHIA J450 TEST DATA (LONG SHROUD WITHOUT NOZZLE)
DATE: 13 JUL 1999
Pamb: 1016 mbar
Temperature: 71^0 F

100% spool speed

ENGINE PORT	ZOC PORT	ZOC PRESSURE(“H_2O)	MANOMETER (“H_2O)
A	1	-0.0181	-1.5
B	2	-0.0482	-7.5
C	3	-0.0475	-8.5
D	4	-0.0597	-4.0
E	5	-0.0340	-7.5
F	6	-0.0531	-8.0
G			-7.5
H			-5.5
I			
J	7	-0.0335	-3.0
K	8	0.0032	-1.0

90% spool speed

ENGINE PORT	ZOC PORT	ZOC PRESSURE(“H_2O)	MANOMETER (“H_2O)
A	1	-0.0136	-1.0
B	2	-0.0236	-5.5
C	3	-0.0395	-6.0
D	4	-0.0577	-3.0
E	5	-0.0382	-5.5
F	6	-0.0441	-6.2
G			-6.0
H			-4.5
I			
J	7	-0.0278	-3.0
K	8	-0.0005	-0.7

80% spool speed

ENGINE PORT	ZOC PORT	ZOC PRESSURE(“H_2O)	MANOMETER (“H_2O)
A	1	-0.0300	-1.0
B	2	-0.0335	-2.5
C	3	-0.0330	-3.0
D	4	-0.0034	-1.8
E	5	-0.0364	-3.5
F	6	-0.0388	-4.0
G			-3.7
H			-3.0
I			
J	7	-0.0307	-2.0
K	8	0.0053	-0.7

APPENDIX F. SHROUD PRESSURE PLOTS

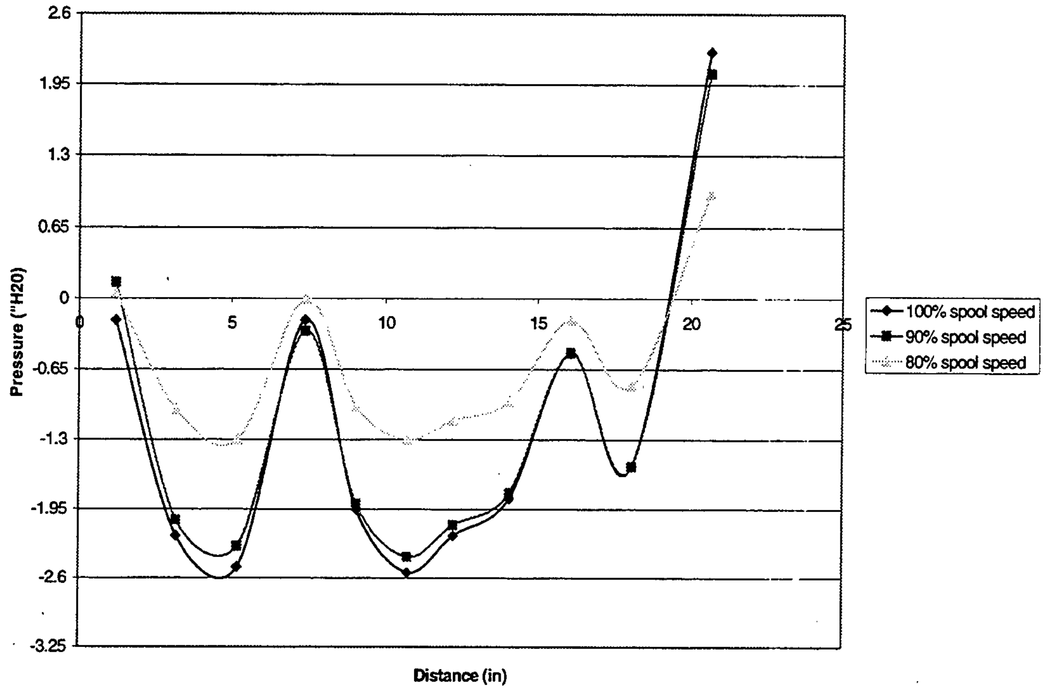

Figure E-1. Short Shroud with Nozzle Pressure Distribution

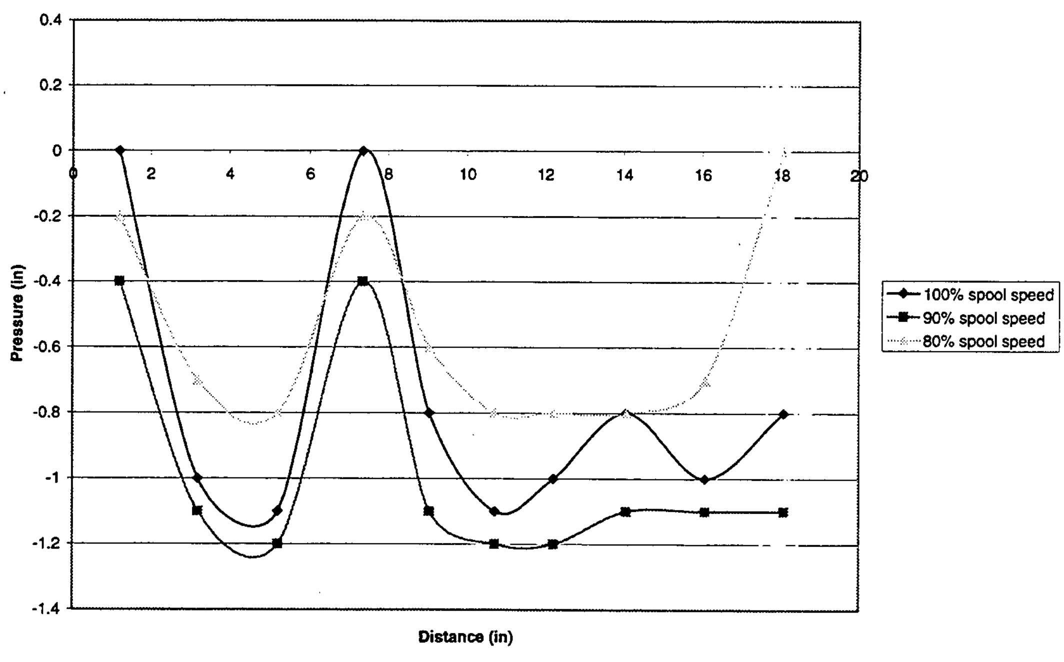

Figure E-2. Short Shroud without Nozzle Pressure Distribution

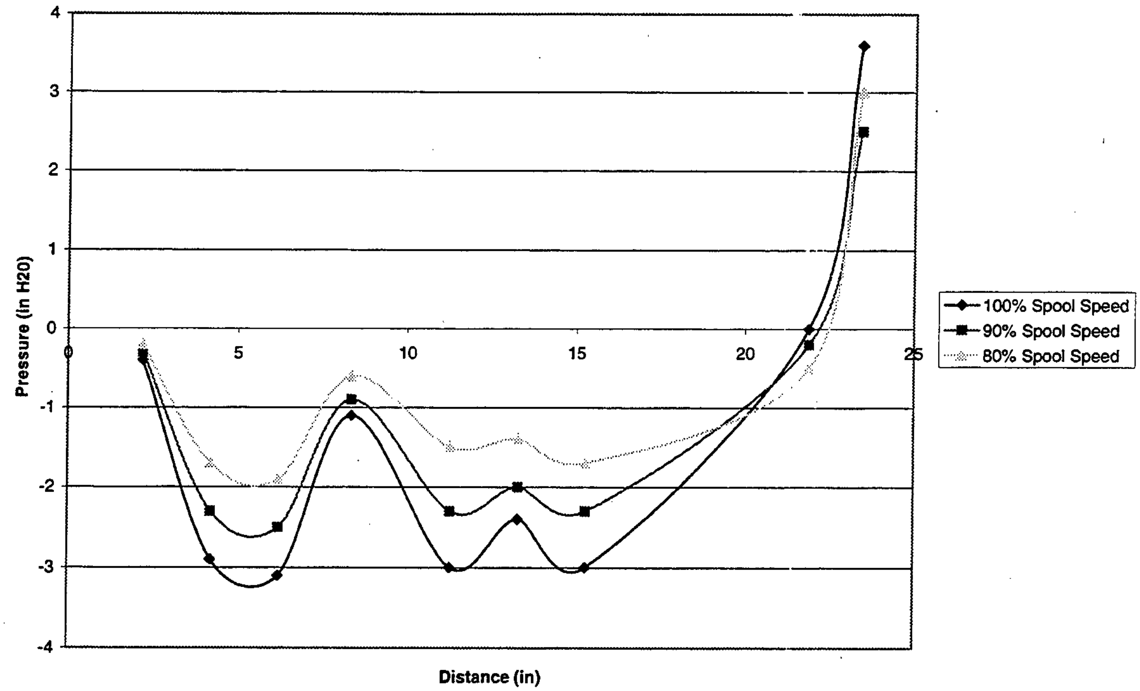

Figure E-3. Medium Shroud with Nozzle and Elliptic Intake Pressure Distribution

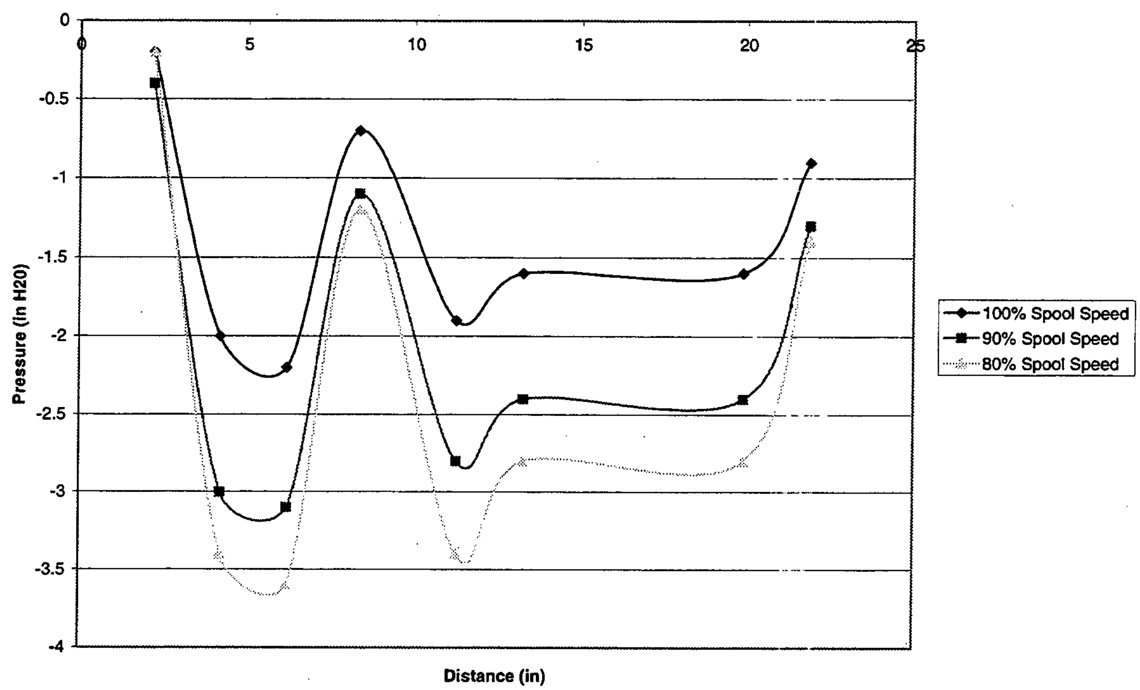

Figure E-4. Medium Shroud with Nozzle Elliptic Intake Pressure Distribution

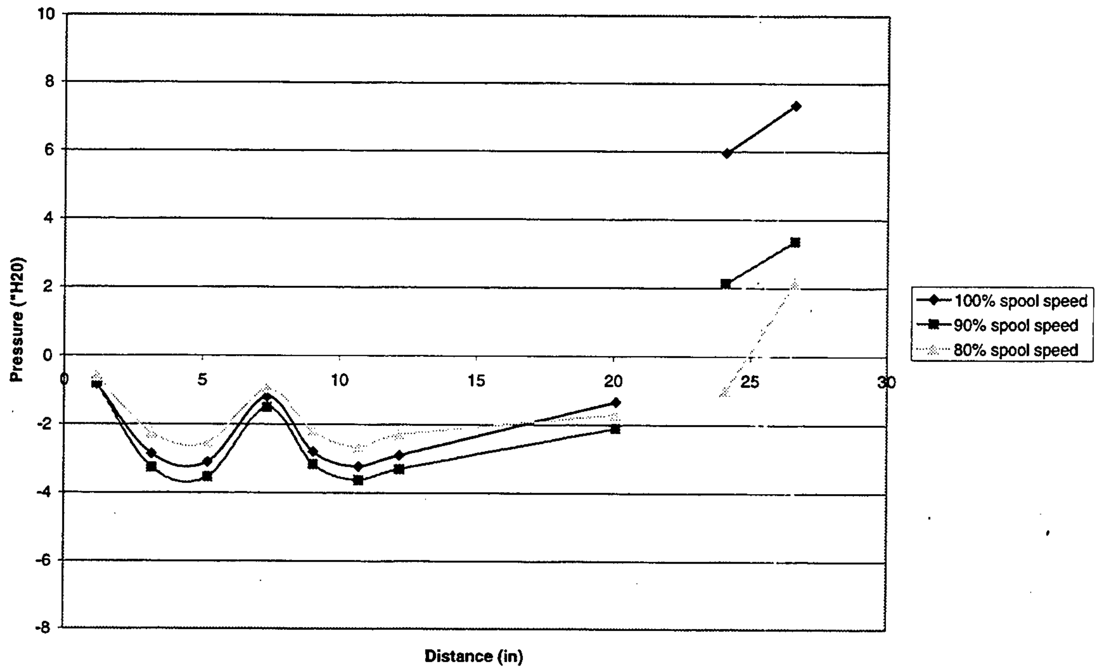

Figure E-5. Long Shroud with Nozzle Pressure Distribution

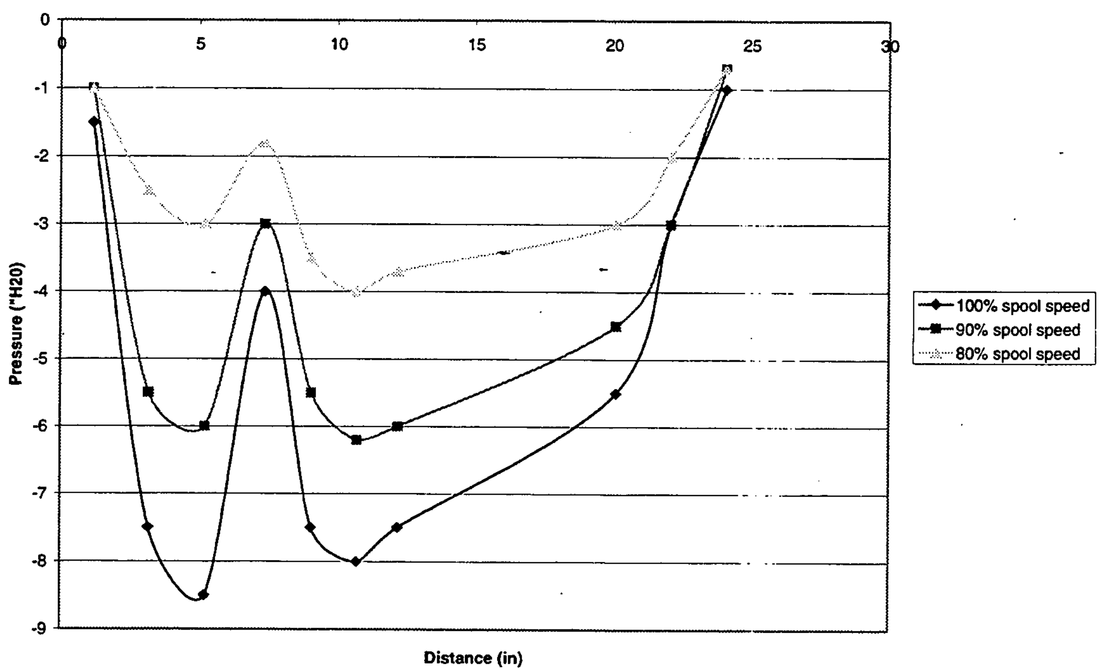

Figure E-6. Lomg Shroud with Nozzle Pressure Distribution

THIS PAGE INTENTIONALLY LEFT BLANK

APPENDIX G. SOPHIA J450 TEST PROGRAM CHECKLIST

G1. FUEL CELL AND THRUST BEAM CHECKLIST

1. Ensure that the test rig is configured in accordance with Figures 1 and 4 and that all devices are properly energized.
2. The fuel pump power supply should be OFF with the voltage knob turned counter clockwise until slight resistance is felt.
3. Zero the thrust beam by connecting the CHANNEL 5 output of the signal conditioner to the DVM front panel. Once properly connected, adjust the ZERO KNOB accordingly until the DVM reads 0 mV. Once zeroed, restore the signal conditioner and DVM to their initial configuration (REAR position).
4. Calibrate the fuel flow beam in the following manner
   4.1. Connect the strain gages (1 and 2) in a half Wheatstone bridge configuration as shown on the inside cover of the P-3500.
   4.2. Set the bridge push button to half-bridge position.

4.3. Depress AMP ZERO and adjust thumbwheel until ±0000 is displayed.

4.4. Depress GAGE FACTOR and ensure the range is set on 1.7-2.5.

4.5. Adjust GAGE FACTOR knob until 2.08 is displayed.

4.6. Depress RUN and set the BALANCE Control for a reading of +0000

4.7. With a DVM connected to the P-3500 output, adjust the OUTPUT thumbwheel until the DVM reads 0 mV.

4.8. Disconnect the external DVM.

4.9. Perform a calibration of Fuel Cell.

5. Place Fuel bottle on carriage and connect fuel line to engine.
6. Prime fuel pump by disconnecting the fuel line forward of the check valve.

G2. DATA ACQUISITION SYSTEM SETUP CHECKLIST

1. Energize the HP9000 computer system.
2. The first screen is the HP9000 Series 300 Computer Data Acquisition/Reduction System introduction.
3. Select F7 and set the current time and date. The format is HH: MM: SS for the time, then select F2 and set the date DD MMM YYYY, (i.e. 10:20:00, 08 Jan 1999).
4. Check ZOC boxes 1-3 are ON.
5. Select F3, Old HP6944A Directory.
6. Select F1, ZOC-14 Module Menu.

7. Open the Nitrogen bottle valve and adjust the pressure reducer at the bottle so that 110 psi is displayed. The pressure reducer on the rear of the CALSYS 2000 should read 90 psi when Nitrogen bottle is energized.
8. Ensure the CALSYS 2000 pressure range on CALMOD 2 are set at 20, 10 and 0 in Hg respectively.
9. Select [F4], Read CALSYS 2000 Calibration Pressures.
10. Select [2] to scan CALMOD.
11. Select [1], for printer and wait until the CALMOND 2 do calibration.
12. Select [F2] to continue, if the high, middle, and low pressures displayed are correct, continue on to the next step. If the calibration pressures are not correct, repeat steps 8 and 9 until correct.
13. Secure Nitrogen to save gas.
14. Select [F1] to Scan 1-3 ZOC-14 Modules (32 ports each). The default program "SCAN-ZOC-08" will initialize.
15. Once "SCAN-ZOC-08" introduction screen is displayed, select the [STOP] key.
16. Select [F5] to LOAD and type "MICROJET".
17. Select [F1] and return to make changes to the equations of fuel-line (2450) and thrust-line (2660).
18. When you put the equations select SHIFT-RESET and then [F8] "MICROJET".
19. Once "MICROJET" is loaded, select [F3] to RUN.
20. Once "MICROJET" introduction screen is displayed select [F3] for system setup.

21. Select 0 for hard drive ":,700" storage.

22. Select 1000 Hz for sampling rate.

23. Select 5 for samples per port.

24. Select 1 ZOC connected to Multi-programmer.

25. Select 3 for the number of desired runs.

26. Select 5 for the time interval (in seconds) between data runs.

27. Select 2 for CALMOD set for ZOC # 2.

28. Turn on the Nitrogen.

29. Select F4 when nitrogen system is energized.

G3. ENGINE STARTUP AND OPERATION CHECKLIST

1. Connect the air-trigger to the J450. Ensure that the air compressor is fully charged before attempting start.
2. Ensure the spark plug is installed correctly. (Gap facing forward)
3. Pre-lube the engine bearings before start.
4. Pre-spin engine to ensure freedom of movement.
5. Engine is now ready for start.
6. Apply start air and once the rotor sound level has increased, push the igniter button.
7. Slowly increase the voltage to the fuel pump by turning the know in the clockwise direction.
8. Fuel pressure should not exceed 1.0 bar on start up.

9. Continue to supply start air until a pressure of at least 0.3 bars in the compressor.

   Adjusting the fuel pump pressure to 0.4 bars should correspond to a compressor pressure of approximately 0.4 bar.

NOTE: If engine does not start within 10 seconds, turn off fuel pump and spark while continuing start air. Once excess fuel and oil is drained attempt restart.

NOTE: If hot start occurs (Tail Pipe Glows red-hot) cut the power to fuel pump immediately but continue ignition and start air. After 5 seconds reenergize fuel pump.

NOTE: If extremely cold, extra Coleman will ensure combustion. Do not exceed recommended ratios.

10. Confirm the flow of lubrication oil immediately after start.
11. The safe operating range is below 1.3 bars. **NEVER EXCEED 1.3 bar compressor pressure**.
12. To cease engine operation, reduce power to 0.7 bars and secure power to the fuel pump.

G4. DATA ACQUISITION SYSTEM CHECKLIST

1. Energize the Nitrogen system and select [F4]

2. Once the engine is operating at the desired speed and stabilized, select F5 to begin data acquisition sequence.
3. Manually record the Thrust and Fuel Flow rate for each of the data runs as displayed on the screen.
4. Once the data collection sequence is completed, secure the engine.
5. Secure Nitrogen once post calibration is complete.
6. Select F6 to begin data reduction.
7. Select F8 to exit once data reduction is complete.
8. Select STOP to display the reduced data.
9. Select F5 and type "READ-MJ-ZOC".
10. Select F3 to RUN.
11. Enter 1, date (YMMDD), Run number. (i.e. for run 1 on 08 March 1999, type: **1,90308,1**).
12. Select 1 for printer option.
13. Select 0 to Exit.

NOTE: Selecting exit does not exit the program but displays the average of the port readings for the selected data run.

14. Select STOP to exit the program.
15. Repeat steps 10-13 for the remaining data runs.

16. If ejector data was measured select STOP.

17. Select F5 and type “EJ_ZOC”.

18. Select F3 to run.

19. Data files are presented in the same manner as above.

20. When complete viewing data select STOP.

21. Type PRINTER IS CRT.

G5. DATA FILE PURGE CHECKLIST

1. The raw data files are stored on the "HP9000 “:,700” hard drive as ZW190381 (example for 08 March 1999, run number 1) through ZW19038X for X data runs.
2. The reduced data files are stored as ZRXXXXXX and the calibrations data is stored as ZCXXXXXX.
3. Select F5 and type "ZOC_MENU".
4. Select F3 to Run.
5. Select F8 to exit menu.
6. Type **MSI ":,700"**.
7. Type PURGE "FILENAME". (ex. PURGE "ZW190381").
8. Ensure deletion of each files. If all created files are not deleted an error will be encountered if obtaining additional data.
9. Cycle the power switch on the lower left corner of the HP9000 CPU to reset the computer.

G6. QUICK REFERENCE CHECKLIST

This checklist guide is provided for convenience and to ensure all systems have been properly configured.

1. Power up: HP9000	______	______
SCANIVALVES (1 & 2)	______	______
ZOC Systems	______	______
2. Perform a visual inspection of engine and test stand	______	______
3. Enter correct date into computer	______	______
4. Place fire bottle within 10 feet of test rig	______	______
5. Perform Calibration of the Thrust Beam	______	______
6. Perform calibration of the Fuel Cell	______	______
7. Load "MICROJET_CAL" to ensure data Acquisition working correctly	______	______
8. Enter corrected slope in "MICROJET" Fuel-line 2450 & Thrust-line 2660)	______	______
9. Place exhaust fan on exhaust duct	______	______
10. Place fuel container on carriage (ensure siphon is down)	______	______
11. Disconnect fuel line aft of check-valve and purge line Do not run pump > 60 seconds dry)	______	______

12. Check all lines for proper connection ______ ______

13. Connect air start line (Ensure water purged from tank) ______ ______

14. Pre-lube engine bearings ______ ______

15. Pre-spin engine to ensure freedom of movement ______ ______

16. Perform a system pressure Calibration (Secure nitrogen after calibration) ______ ______

17. Load "MICROJET" and input parameters(Press F4 after nitrogen re-energized) ______ ______

18. Power supply energized for:
    Spark Igniter ______ ______
    Fuel Pump
    Exhaust Fan

19. Start Engine and stabilize (Press F5 after stabilized) ______ ______

20. Manually record Thrust and Fuel Flow ______ ______

21. Secure engine and fuel pump power ______ ______

22. Secure nitrogen after post calibration complete ______ ______

23. Reduce data and view output files (As desired) ______ ______

24. Purge Data Files ______ ______

25. For additional data runs repeat step 12 through 22 ______ ______

THIS PAGE INTENTIONALLY LEFT BLANK

APPENDIX H-1. INTAKE DESIGNS

Although the aircraft manufacturer, usually designs the intake, it becomes very important to the overall jet engine thrust output. The faster the airplane goes, the more critical the inlet design becomes. Engine thrust will be maximized if the intake supplies the engine with the required airflow at the highest possible pressure. The intake must also allow the engine to operate over wide variations in angle of the attack and yaw.

For supersonic aircraft, the intake should not produce strong shock waves or flow separations and should be of minimum weight for both subsonic and supersonic designs. Inlet ducts add to the parasite drag, or aerodynamic resistance drag. Parasite drag can be broken down into skin friction due to the viscosity of the air, form drag due to the shape of the duct and interference drag that comes from the junctions of the aircraft and engine components.

The inlet duct must operate from static conditions up to high aircraft Mach numbers with a high duct efficiency at all altitudes. Inlet ducts should be straight and smooth as possible and should be designed in such a way that the boundary layer blockage will be held to a minimum. The length, shape, and placement of the duct are determined to a great extent by the location of the engine in the aircraft. Not only must the duct be large enough to supply the proper airflow, but also it must be shaped correctly to deliver the air to the front of the compressor with an even pressure distribution.

Another primary task an inlet duct must do during flight operations is to convert the kinetic energy of the rapidly moving inlet airstream into a ram pressure rise inside the duct. To do this it must be shaped so that the air flow velocity is slowly and smoothly decreased, while the ram pressure is slowly and smoothly increased.

Inlet ducts are rated in two ways: the duct pressure ratio and the ram recovery pressure. The duct pressure efficiency ratio is defined as the ability of the duct to convert the kinetic or dynamic pressure energy at the inlet of the duct into static pressure energy at the inlet of the compressor, without a loss in total pressure. The ram recovery pressure is that aircraft speed at which the ram- pressure rise is equal to the friction losses, or that airspeed at which the compressor inlet total pressure is equal to the outside ambient air pressure.

It is interesting to note that the engine manufacturers rate their engines using a bellmouth inlet. This type of inlet is essentially a bell- shaped funnel having carefully rounded shoulders, which offer practically no air resistance. The duct loss is so small that it is considered zero and engine performance data can be gathered without any correction for inlet duct loss being necessary.

APPENDIX H-2. CALCULATION OF INTAKE MACH NUMBER

Two programs were written in MATLAB to generate the Mach number in front of the engine intake for subsonic and supersonic flow.

```
function [f]=fox(x)
mdot=0.256;
area=(pi*(2.33)^2/4)/144;
R=54.4;
gc=32.2;
gam=1.4;
pt=144*18.745;
Tt=556.01;
f=mdot/area-pt*sqrt(gam)*x/sqrt(R*Tt)*(1/(1+(gam-
1)*x*x/2))^((gam+1)/(2*(gam-1)));
```

```
a=0;
b=1;
eps=0.00001;
foa=fox(a);
fob=fox(b);
iter=0;
if (foa*fob)<0
   while ((abs(b-a)>eps) & (iter<100))
      m=(a+b)/2;
      fom=fox(m);
      if (foa*fom)<0
         b=m;
      else
         if (fom*fob)<0
            a=m;
         else
            disp('The iteration process did not converge.');
         end
      end
      iter=iter+1;
   end
   disp('The root of f(x) is '),m
   disp('Number of iterations = '),iter
else
   disp('There is no root in [a,b].');
end
```

THIS PAGE INTENTIONALLY LEFT BLANK

APPENDIX I. CALCULATION FOR ENGINE CONFIGURATION CENTER OF GRAVITY

A program was written in MATLAB to calculate the center of gravity for different engine configurations.

```
disp('First part - long shroud');r=2.935;
R=3.5;
ro=0.28978;
t=0.095;
mass1=ro*pi*(R*R-r*r)*t;
mass2=2*mass1
r=2.185;
R=2.75;
mass3=ro*pi*(R*R-r*r)*t
mass4=2*mass3
W1=2.25112;
Xcg1=3.3;
W2=0.76442;
R=2.25;
r=3.0;
l=3.085;
a=(R-r)/l;
z=0.065;
Xcgi2=(a*l*l/3+(r-z/2)*l/2)/(a*l/2+(r-z/2))
Xcg2=Xcgi2+6.6+0.095
W3=0.67771;
Xcg3=11.4725;
W4=1.37771;
Xcg4=16.07;
W5=1.36771;
Xcg5=22.075;
W6=0.55886;
R=1.581;
r=2.25;
l=2.935;
a=(R-r)/l;
z=0.065;
Xcgi6=(a*l*l/3+(r-z/2)*l/2)/(a*l/2+(r-z/2))
Xcg6=Xcgi6+6.6+3.275+3.195+6.02+6.01+0.095
Wa=mass1;
Xcga=0.095/2;
Wb=mass2;
Xcgb=6.6;
Wc=mass4;
Xcgc=6.6+3.275;
Wd=mass4;
Xcgd=6.6+3.275+3.195;
We=mass4;
Xcge=6.6+3.275+3.195+6.02;
```

```
Wf=mass4;
Xcgf=6.6+3.275+3.195+6.02+6.01;
Weng=3.82;
Xcgeng=4.75;
num1=Xcg1*W1+Xcg2*W2+Xcg3*W3+Xcg4*W4+Xcg5*W5+Xcg6*W6;
num2=Xcga*Wa+Xcgb*Wb+Xcgc*Wc+Xcgd*Wd+Xcge*We+Xcgf*Wf;
den1=W1+W2+W3+W4+W5+W6;
den2=Wa+Wb+Wc+Wd+We+Wf;
Wtwoe=den1+den2
Xcgwoe=(num1+num2)/(den1+den2)
Wtwe=den1+den2+Weng
num1=num1+Xcgeng*Weng;
den1=den1+Weng;
Xcgwe=(num1+num2)/(den1+den2)

disp('Second part - short shroud');
Xcg6=Xcgi6+6.6+3.275+3.195+6+0.095
num1=Xcg1*W1+Xcg2*W2+Xcg3*W3+Xcg4*W4+Xcg6*W6;
num2=Xcga*Wa+Xcgb*Wb+Xcgc*Wc+Xcgd*Wd+Xcge*We;
den1=W1+W2+W3+W4+W6;
den2=Wa+Wb+Wc+Wd+We;
Wtwoe=den1+den2
Xcgwoe=(num1+num2)/(den1+den2)
Wtwe=den1+den2+Weng
num1=num1+Xcgeng*Weng;
den1=den1+Weng;
Xcgwe=(num1+num2)/(den1+den2)
```

APPENDIX J. CALIBRATION CURVES

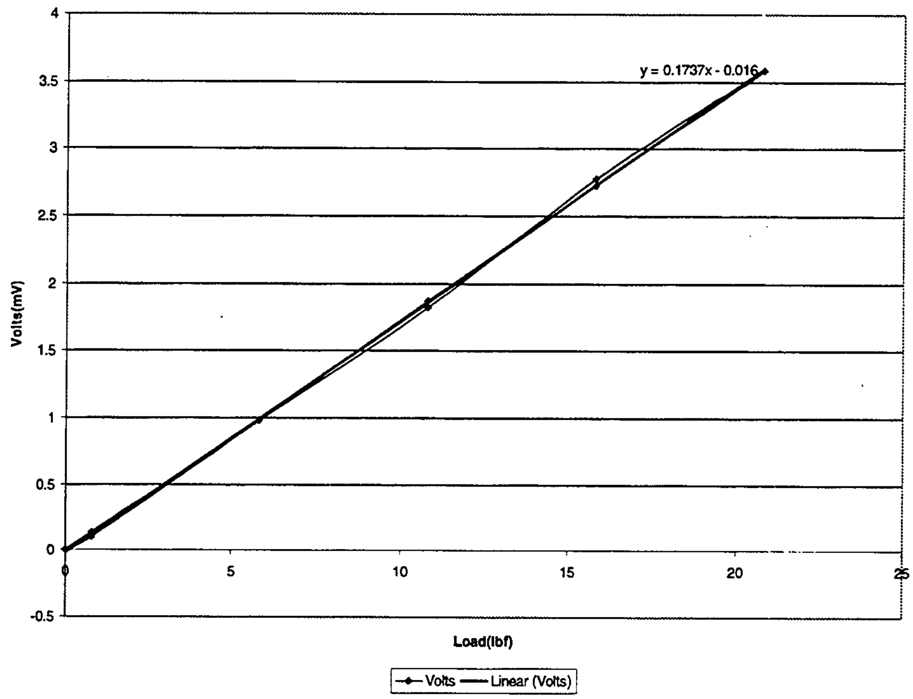

Figure J-1. Thrust Beam Calibration (22 JUL 99)

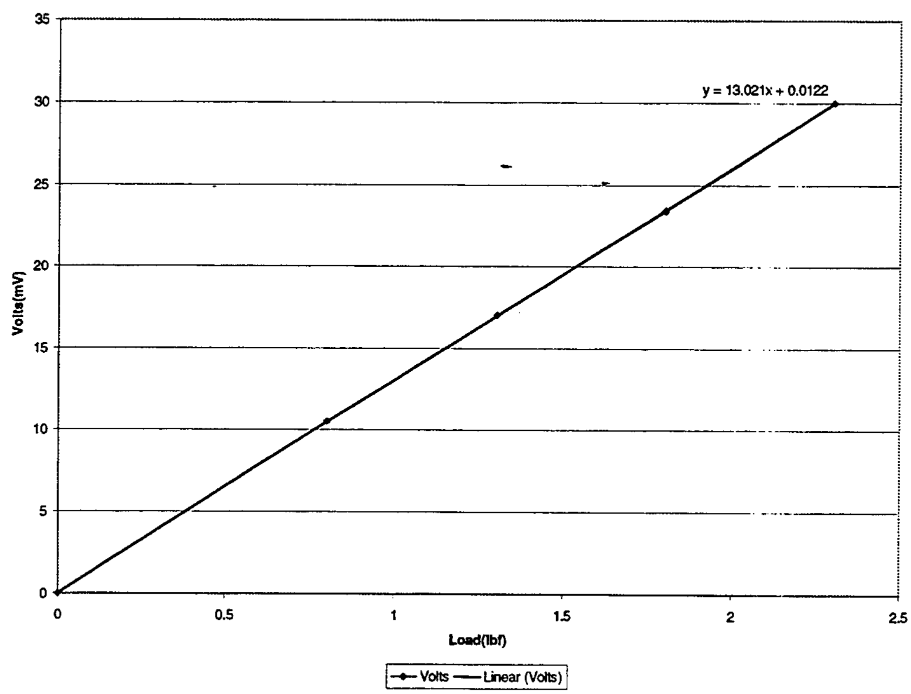

Figure J-2. Fuel Weight Calibration Measurement (22 JUL 99)

THIS PAGE INTENTIONALLY LEFT BLANK

LIST OF REFERENCES

1. Rivera, G., *Turbochargers to Small Turbojet Engines for Uninhabited Aerial vehicles*, Engineer's Thesis, Department of Aeronautics and Astronautics, U.S. Naval Postgraduate School, Monterey, CA, June, 1998

2. Lobik, L.P., *Unmanned Aerial Vehicles: A Study of Gas Turbine Application*, Master's Thesis, Department of Aeronautics and Astronautics, U.S. Naval Postgraduate School, Monterey, CA, September 1995

3. Kurzke, J., *GASTURB 7.0 for Windows, A Program to Calculate Design and Off-Design Performance of Gas Turbines*, 1996

4. Hackaday, G.L.., *Thrust Augmentation For a Small Turbojet Engine*, Master's Thesis, Department of Aeronautics and Astronautics, U.S. Naval Postgraduate School, Monterey, CA, June, 1998

5. Sophia USA, *Sophia J450 Turbine Engine Instruction Manual and Owner's guide*

6. Hill, P.G., and Peterson, C.R., *The Mechanics and Thermodynamics of Propulsion*, Addison-Wesley Publishing Company, Inc., June 1992

THIS PAGE INTENTIONALLY LEFT BLANK

INITIAL DISTRIBUTION LIST

1. Defense Technical Information Center 2
   8725 John J. Kingman Rd., Suite 0944
   Ft. Belvoir, VA 22060-6218

2. Dudley Knox Library 2
   Naval Postgraduate School
   411 Dyer Rd.
   Monterey, CA 93943-5101

3. Prof. Gerald H. Lindsey, Code AA/Li.. 1
   Chairman, Department of Aeronautics and Astronautics
   Naval Postgraduate School
   699 Dyer Road, Room 137
   Monterey, CA 93943-5106

4. Prof. Garth V. Hobson, Code AA/Hf 5
   Department of Aeronautics and Astronautics
   Naval Postgraduate School
   699 Dyer Road, Room 137
   Monterey, CA 93943-5106

5. Prof. Raymond P. Shreeve, Code AA/Sf... 1
   Department of Aeronautics and Astronautics
   Naval Postgraduate School
   699 Dyer Road, Room 137
   Monterey, CA 93943-5106

6. Naval Air Warfare Center – Aircraft Division
   Propulsion and Power Engineering
   22195 Elmer Road
   Patuxent River, MD 20670-5305
   ATTN: J. Carroll, Code 4.4.3.2, BLDG 1461 1
   C. Georgio, Code 4.4.. 1

7. Andreou Loukas 1
   7 Marathonos St.
   18900 Salamis, GREECE